RUDDER ROLL REDUCTION FOR SMALL SHIPS

by

Christopher Robert Martin

B.A.Sc., The University of British Columbia, 1989

A THESIS SUBMITTED IN PARTIAL FULLFILLMENT OF THE

REQUIREMENTS FOR THE DEGREE OF

MASTER OF APPLIED SCIENCE

in

THE FACULTY OF GRADUATE STUDIES

DEPARTMENT OF MECHANICAL ENGINEERING

We accept this thesis as conforming

to the required standard

THE UNIVERSITY OF BRITISH COLUMBIA

April 1993

In presenting this thesis in partial fulfilment of the requirements for an advanced degree at the University of British Columbia, I agree that the Library shall make it freely available for reference and study. I further agree that permission for extensive copying of this thesis for scholarly purposes may be granted by the head of my department or by his or her representatives. It is understood that copying or publication of this thesis for financial gain shall not be allowed without my written permission.

(Signature)

Department of _Mech. Eng._

The University of British Columbia
Vancouver, Canada

Date _93/04/29_

Abstract

Roll motion on a ship can be very uncomfortable, and in the extreme, dangerous. It is possible to use the rudder to reduce roll motion as has been demonstrated by others on naval and coast guard vessels. For this study, five controllers were chosen and designed to implement a rudder roll reduction system as part of an autopilot on a fishing vessel. A numerical model and a physical model were prepared for testing these controllers. The results from the numerical model indicate rudder roll reduction does not work for the fishing vessels tested. These results are suspect for several reasons.

Table of Contents

List of Tables

List of Figures

Nomenclature

This report covers two engineering areas, each with its own symbol standards. Therefore, two nomenclature listings are provided, one for control and one for naval architecture. There is some cross-over, for example ϕ is used for roll angle in both control discussion and naval architecture discussion.

Control Nomenclature

$\mathbf{A}$ — system matrix

$A(z^{-1})$ — system polynomial

$\mathbf{B}$ — input matrix

$B(z^{-1})$ — input polynomial

$\mathbf{C}$ — output matrix

$\mathbf{G}$ — sliding surface coefficients

$\mathbf{H_{Nu}}$ — predicted output response

J — cost function

K — arbitrary gain

$\mathbf{K}(t)$ — gain matrix in AML

K_r — roll weight

K_{ry} — roll velocity weight

K_y — yaw velocity weight

N — prediction horizon

N_u — control horizon

$\mathbf{P}(t)$ — covariance matrix in

AML

$\mathbf{S}(k)$ — sliding surface

$s(k)$ - ideal set-point

T_D — derivative time constant

T_I — integral time constant

T_ϕ - roll natural period

T_ψ - yaw rate time constant

$\tilde{u}$ — vector of future controls

$\mathbf{x}$ — state vector

α — EFRA factor

β — EFRA factor

δ — EFRA factor

ϵ — boundary layer thickness

$\eta(t)$ — a posteriori errors

$\mathbf{\Theta}$ — estimated parameters

λ — EFRA exponential forgetting factor

ϕ — roll angle

$\mathbf{\Psi}$ — predicted response

Ψ_0 — predicted free response

ψ — yaw angle

Naval Architecture Nomenclature

A_R — area of rudder

B — ship's beam

b — linear roll damping

C_B - block coefficient

D — moulded depth

F_n - Froude Number

GM_T — effective metacentric height

g - gravitational acceleration

H_W - significant wave height

I_{xx} — roll mass moment of inertia

I_{zz} — yaw mass moment of inertia

J_{xx} — added roll mass moment of inertia

J_{zz} — added yaw mass moment of inertia

K_H — hydrodynamic roll moments

K_R — rudder roll moment

K_W — wave excited roll moment

L — ship length

m — ship mass

m_x — added mass in the x direction

m_y — added mass in the y direction

N_H — hydrodynamic yaw moments

N_R — rudder yaw moment

N_W — wave excited yaw moment

r — yaw rate

T,d — mean draught

u — surge velocity

V - ship's velocity

v — sway velocity

Y_H — hydrodynamic sway forces

Y_R — rudder sway force

Y_W — wave excited sway force

z_R - vertical distance from c.g. to rudder.

α_R — effective rudder in-flow angle

Δ — ship's displacement

δ - rudder command angle

ζ — roll damping ratio

x

ξ — wave slope amplitude

λ — rudder aspect ratio

ρ — density of sea water

τ — trim

χ — heading angle

relative to waves

ω — wave frequency

ω_e — wave encounter

frequency
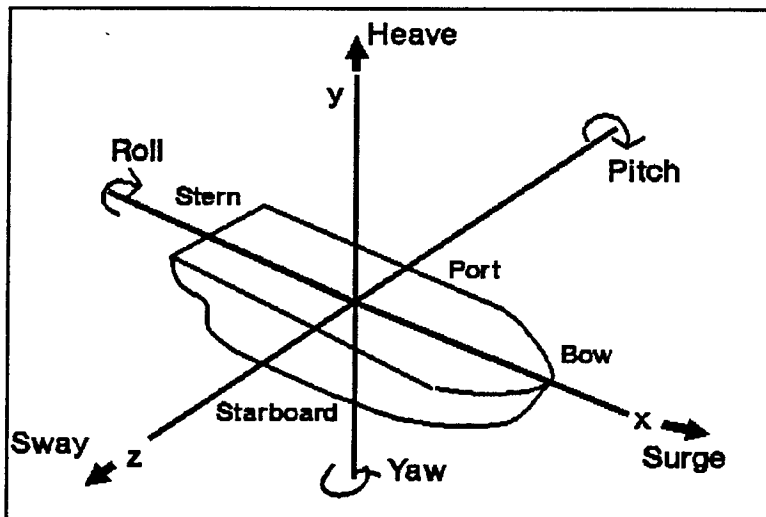
Figure 1. Ship geometry and motions

Part 1: Introduction

Rolling is one of six motions that all ships experience. As rolling becomes more pronounced, it affects both the crew and the vessel. Rolling reduces task proficiency and both directly and indirectly increases the risk of injury. The ship's fittings, such as machinery mounts and cargo holding structures and systems, must resist the resulting forces. Excessive motion can lead to capsize, an endangerment of both life and vessel. By decreasing roll motion, not only is the comfort level increased, but safety is also increased.

There are many methods available to decrease roll motion, though all are not currently used. All methods increase roll damping, thereby reducing the dynamic amplification at resonance of the roll motion. They can be divided into two types: passive and active.

The most common passive stabilizing devices are bilge keels, which are fitted on most round bilged boats, but rarely on hard chined vessels. Bilge keels work through viscous effects and vortex shedding at very low speeds. As the speed of the boat increases, a hydrodynamic lift begins to act, generating an opposing roll moment.

Less common passive devices are passive roll tanks. Roll tanks are designed to dampen the roll motion by having water slosh

inside them 90 degrees out of phase of the roll motion. However, they add weight, take up cargo space and reduce overall stability, because they reduce the metacentric height. Roll tanks are rarely used on local fishing vessels.

Two passive devices that are used locally in the Pacific Northwest are paravanes and batwings. Paravanes are triangular sheets of wood or metal that are hung in the water from poles extending laterally outward from the boat. They work by alternately diving downward when the pole to which they are attached rises, producing an opposing roll moment. Paravanes are often found on trawlers because of the existing poles used in the trawling process.

The last passive devices are batwings, which work in much the same way as bilge keels. Batwings are sheets of metal perpendicular to and extending laterally outward from the keel. They decrease the roll through vortex shedding and, at higher forward speeds, through dynamic lift. However, they also increase the resistance of the vessel.

The second type of stabilizers used to decrease roll motion are active stabilizers. Active systems are characterized by sensors, controllers, and actuators.

Active tanks are one type of active stabilizers. Active tanks work on much the same principle as passive tanks; however, a sensor is used to tell a pump when and which way to move the

water. An active tank system results in the use of smaller tanks, and therefore little loss in stability and active tanks can be used in a wide range of conditions. The disadvantage is the weight and size of the pump necessary and the energy required to operate the pump.

Another type of active damper are fins, which protrude from the hull . A sensor measures the direction and speed of the roll and the fins' angles are adjusted to produce an opposing roll moment. The disadvantages of fins are they are vulnerable to damage, ineffective at low speeds, and in large motions can stall, producing little lift and little opposing roll moment.

The rudder, with which almost every ship is fitted, is usually placed below the centre of gravity of the ship. The lift force of the rudder acts below the roll centre of the ship, producing a roll moment. Because the ship's speed of response in roll is much faster than that in yaw, a control scheme has been implemented on some vessels, which reduces the roll without affecting yaw.

1.1 Problem

The primary problem is to develop a rudder roll reduction autopilot with applicability to a broad range of small vessels. Because the autopilot is for small vessels, secondary characteristics (problems) that should be considered are:

3

-the autopilot should be cost effective for the small

 vessel's owner.

-the sensors necessary should be inexpensive and few.

-there should be no major alteration to the steering gear.

1.2 Scope & Assumptions

The control system that was explored in this thesis is a rudder roll reduction system as part of an autopilot. A number of controllers were selected and then evaluated.

The system has one input, the rudder, and two outputs, roll and yaw. On all boats the rudder has a maximum angle, in either direction, which it can rotate from the centre line (zero degrees). For the craft considered here, the rudder has a set constant slew rate. It is understood that the constant slew rate is slow, which was factored into the design. It was assumed that the rudder provides sufficient roll moment at forward speed necessary for roll reduction.

This one input, two output system to be designed for is a Single Input Multi Output (SIMO) system. Some of the major criteria for the controllers are:

 - the same controller must be able to be used on different

 boats easily.

 - work on one boat under different loading conditions

 (parameter variations).

4

- the controllers must work on real boats, whose motions are non-linear.
- the controllers must work with the presence of wind and waves affecting the vessel (coloured noise).
- the controller must take into account the rudder limitations (maximum angle and constant slew rate).

The project did not cover all the aspects of autopilot design. The autopilot served only as a regulator, that is, for course keeping only. No mention will be made of turning or manoeuvring. In addition, the possibility of helmsman steering with a rudder roll reduction system also acting was not explored.

All controllers have "tuning knobs" for which adjustments can be made to improve the controller's response to different stimuli. This project did not address the tuning of each controller for different, specific tasks. All controllers were tuned using the same test and specified response. The parameters remained fixed through all tests.

All design was done in discrete time, that is, using difference equations instead of differential equations and the accompanying analytical tools such as z-domain analysis. The process was linearized for controller design. It was modelled as an Auto-Regressive Moving Average (ARMA) or a state space process. The coloured noise was modelled as an ARMA process driven by white noise.

The vessels designed for in this project are in some ways much
different than the vessels dealt with in the literature [1-7][*].
Previous controllers were designed for and tested on much larger
vessels such as naval vessels. Also, most design information and
qualitative discussion of transverse motions in standard
literature [20,21] are related to larger vessels.

1.3 General Approach.

Controllers were chosen and designed. Their parameters were set
using one evaluation criteria for all designs. The first
controller designed was of the same form and specifications of
autopilots currently on the market. Its responses were used as
the baseline against which the other controllers' responses were
measured. All controllers were first designed as autopilots
alone, then as roll reducing autopilots to see what effect the
addition of roll reduction had on the ship response.

The controllers were first tested in numerical simulations. Here
their responses to specific environments and process parameter
variations were examined.

The controllers were then to be tested on a physical model. Here
their responses to a real physical environment with all its
associated non-linearities , noise from different sources, and

_____

[*]Numbers refer to entries in the bibliography .

other peculiarities, were to be examined. The model tests were to be the more accurate test of whether a rudder roll reduction system would work with fishing and other similar sized boats.

At the end of each testing section, the responses of each controller are compared and discussed.

Finally, conclusions and recommendations are made.

1.4 Literature Review

The first research into rudder roll reduction was undertaken in the mid-seventies, using analog controllers. These controllers were tested using scale model and full scale tests. The types of vessels were fast container ships and naval craft. They achieved limited success.

In 1981, Kallstrom [7] conducted a detailed study of a rudder and fin roll control system.

Throughout the 1980's van Amerongen [2,3] and various coworkers carried on an extensive project on rudder roll reduction. Their controller was based on Linear Quadratic Gaussian (LQG) design. The weighting factors in the LQ design were adjusted on line; however, there was no on line ship parameter estimation. They designed an automatic gain control system to compensate for the limited slew rate of the rudder. The testing was broad,

encompassing mathematical models, analog modelling, scale modelling and, full scale trials.

In the 1980's, other researchers, such as Katebi et al.[4], investigated rudder roll reduction using LQ control.

The amount of roll reduction reported in these papers ranged between eight and fifty percent.

None of these researchers used on-line parameter estimation. Except for van Amerongen et al., there was no consideration of rate saturation. All of the vessels investigated were large container vessels or naval vessels.

Part 2: Design Process

2.1 System

The system consists of four major components, shown in Figure 2. The components are the ship itself (or the plant), the rudder, the controller, including sensors, and the external environment. All of these components affect the ship motions of interest: yaw and roll. The ship affects itself through the propeller, which can affect yaw through "prop walk," and by the way it is loaded.
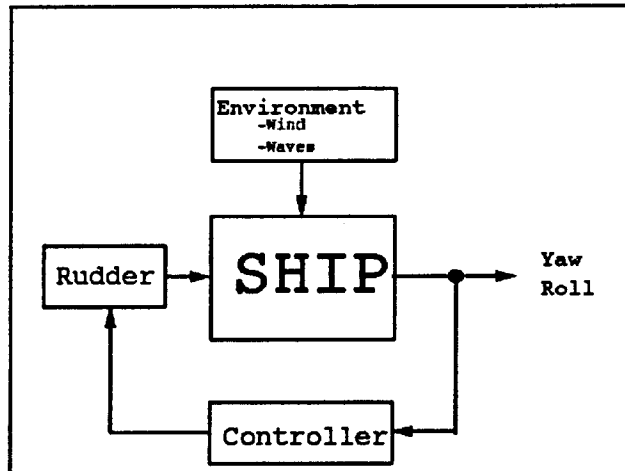
Figure 2. System Diagram

The autopilot is implemented to keep a steady course. It must compensate for external and internal disturbances by using the rudder. The ability to damp roll motions is to be added into the design of the autopilot. That is, the autopilot not only must keep a steady course, but it must also decrease the roll motion.

Important characteristics of the system that will affect the design are as follows:

- The ship is either neutrally stable or unstable in yaw. Neutrally stable means the ship will hold a course, but the slightest disturbance will send the ship off course, and unstable means the ship cannot hold a course on its own.

- The ship is always stable in roll, which means when it is disturbed it will always settle to a steady value. The roll to rudder response is non-minimum phase. In other words when the rudder is moved to one side of neutral, the ship initially rolls in one direction but finally settles in the other.

- The yaw virtual moment of inertia of a typical west coast fishing boat is five to six times larger than the roll moment of inertia.

- There is cross coupling between the motions, that is, roll affects yaw and yaw affects roll. It was expected that yaw would be influenced by roll much less than it influences roll.

- The yaw and roll characteristics will change with speed and loading. Speed is a factor because not only does it change the effectiveness of the rudder, but it also affects the characteristics of the ship.

10

- The rudder is controlled by a hydraulic actuator, which moves at a fixed speed. This can cause difficulties and even instabilities in a roll reduction system, because the rudder angle starts to lag behind the desired angle to such an extent that it starts to increase roll motions.

- It is expected that the controllers will be implemented using a digital processor in commercial production. Although the computational speed of computers have increased tremendously over the years, there are still economic factors to be considered. Therefore, some attention will be paid to the computational effort required.

- The environmental disturbances are usually caused by wind and waves. The disturbances can be constant such as a steady wind, narrow-band random (usually waves), or wide-band random such as wind gusts.

2.2 Detailed Design

The ship will be modelled in a general manner, i.e., using general coefficients rather than specific values. This will be followed by the controller design in the same general manner, i.e., using general coefficients.

The ship was modelled as a linear discrete time Single Input Multi Output System (SIMO). Each motion, roll and yaw, was

modelled as a second order Auto Regressive Moving Average (ARMA) system using difference equations:

$$A(z^{-1}) = \sum_{i=1}^{2} B_i(z^{-1}) \qquad \textbf{(1)}$$

where i=1 is the rudder input

i=2 is the cross-coupling of the motions.

For yaw

$$(1 + a_1 z^{-1} + a_2 z^{-2}) \psi = b_1 z^{-1} u + b_2 z^{-1} \phi \qquad \textbf{(2)}$$

and for roll

$$(1 + a_1 z^{-1} + a_2 z^{-2}) \phi = b_1 z^{-1} u + b_2 (z^{-1} - z^{-2}) \psi \qquad \textbf{(3)}$$

Note that the a_i and b_i are not the same for the two equations.

A standard linear representation in naval architecture for the transverse motions (roll, yaw, and sway) of vessels is a SIMO

state space system:

$$\dot{x} = A_c x + B_c u \qquad\qquad (4)$$

with states:

$$x = \begin{bmatrix} \psi \\ \dot{\psi} \\ v \\ \phi \\ \dot{\phi} \end{bmatrix}$$

where ψ=yaw angle, v=sway velocity, and ϕ=roll angle and u is the rudder angle.

Sway is often ignored because it is difficult to measure, as are the roll and yaw velocities. They could be estimated by using such methods as Kalman Filtering; however, because the plant parameters are estimated, doing both was felt to be too computationally expensive.

Combining the ARMA difference equations into a state space SIMO system, we obtain:

$$x(k+1) = A x(k) + B u(k) \qquad\qquad (5)$$

with states

$$x(k) = \begin{bmatrix} \psi(k) \\ \psi(k-1) \\ \phi(k) \\ \phi(k-1) \end{bmatrix}$$

13

The elements of **A** are the coefficients of $A(z^{-1})$ and $B_2(z^{-1})$ polynomials for each of roll and yaw. The **B** elements consist of the $B_1(z^{-1})$ polynomial. That is:

$$A = \begin{bmatrix} a_{1y} & a_{2y} & b_{2y} & 0 \\ 1 & 0 & 0 & 0 \\ b_{2r} & -b_{2r} & a_{1r} & a_{2r} \\ 0 & 0 & 1 & 0 \end{bmatrix} \qquad B = \begin{bmatrix} b_{1y} \\ 0 \\ b_{1r} \\ 0 \end{bmatrix}$$

where the y and r subscripts indicate the co-efficient are from the yaw and roll difference equations respectively.

Because of the fixed slew rate of the rudder, it is convenient to change the input to Δu and augment the states with $u(k)$. That is:

$$x(k) = \begin{bmatrix} \psi(k) \\ \psi(k-1) \\ \phi(k) \\ \phi(k-1) \\ u(k) \end{bmatrix}$$

The system matrices are now :

$$A = \begin{bmatrix} a_{1y} & a_{2y} & b_{2y} & 0 & b_{1y} \\ 1 & 0 & 0 & 0 & 0 \\ b_{2r} & -b_{2r} & a_{1r} & a_{2r} & b_{1r} \\ 0 & 0 & 1 & 0 & 0 \\ 0 & 0 & 0 & 0 & 1 \end{bmatrix} \qquad B = \begin{bmatrix} b_{1y} \\ 0 \\ b_{1r} \\ 0 \\ 1 \end{bmatrix}$$

After the plant was modelled, the controllers were chosen. A controller must meet the following criteria:

14

1. be able to compensate non-minimum phase plants.

2. be able to compensate open loop unstable plants.

3. work with or be extendable to multivariable plants.

4. work reasonably well in the presence of "coloured" disturbances.

5. handle large parameter variations.

6. handle a control input (actuator) that has a fixed rate.

7. handle a control input that has amplitude limits.

2.3 Parameter Identification

Most controllers' parameters are based on the plant's parameters. To adapt to different plants and to plants under different operating conditions, some controllers use the method of on-line parameter estimation. In other words they estimate the plants' parameters using previous values of the output and the control input, then calculate the next control input.

For the controllers in this thesis that require an on-line parameter estimation algorithm, the algorithm used was Approximate Maximum Likelihood, with some modifications. The algorithm and modifications are summarized here. More detail can be found in Appendix I.

Approximate Maximum Likelihood was chosen because it has good convergence properties and is easily extendable to the case of a

plant with a coloured noise disturbance. It has the form of

$$P(t+1) = P(t) - \frac{P(t) x_I(t+1) x_I^T(t+1) P(t)}{1 + x_I^T(t+1) P(t) x_I(t+1)}$$

$$K(t+1) = \frac{P(t+1) x_I(t+1)}{1 + x_I^T(t+1) P(t) x_I(t+1)}$$

$$\Theta(t+1) = \Theta(t) + K(t+1) \left[y(t+1) - x_I^T(t+1) \Theta(t) \right]$$

where P is the covariance matrix, x_I is the data vector, and θ is a vector of the parameters being estimated.

The first modification is to add an Exponential Forgetting and Resetting Algorithm (EFRA) [8]. This algorithm increases the stability of the AML when excitation is poor (i.e., little or no change in the control input) and tracks time varying parameters. The AML is modified by :

$$P(t+1) = \frac{1}{\lambda} - \frac{\alpha P(t) x_I(t+1) x_I^T(t+1) P(t)}{1 + x_I^T(t+1) P(t) x_I(t+1)} + \beta I - \delta P^2(t)$$

$$K(t+1) = \frac{\alpha P(t+1) x_I(t+1)}{1 + x_I^T(t+1) P x_I(t+1)}$$

The major difference between the EFRA and the usual AML algorithms is in the equation for the covariance matrix. The first two terms correspond to the standard AML with exponential forgetting. The third term provides a lower bound for P, while the last term provides an upper bound.

In this multivariable case, the two subsystems will be identified separately. That is, the coefficients in (2) will be identified, then the coefficients in (3) will be identified.

16

The second modification is a simplification of the coefficients in the yaw subsystem (2). The fact ψ is the integral of $\dot{\psi}$, with respect to time; that is, a pure integrator, will be taken advantage of. Here a_1 is equal to $(-1-a_2)$. Therefore, it is only necessary to identify a_2, which can be done easily (see Appendix I).

2.4 PID Controller

The Proportional-Integral-Derivative controller would not normally be chosen as a controller because it is used more in tracking applications than for regulation, it is difficult to design for multivariable systems, and it cannot be modified to handle a fixed rate control input. However, since it is the industry standard for autopilots, a PID controller using the industry standard parameters will be implemented.

The control algorithm is:

$$u(k) = q_0 y(k) + q_1 y(k-1) + q_2 y(k-2) + u(k-1)$$

$$\text{where} \quad q_0 = K(1 + \frac{T_D}{T_o})$$

$$q_1 = -K(1 + 2\frac{T_D}{T_o} - \frac{T_o}{T_I})$$

$$q_2 = K\frac{T_D}{T_o}$$

The standard values [28,29] for the gain K are 1:0.5 to 1:1, the derivative time constant T_D is 0.25 to 0.5 seconds, and the

integral time constant T_I is 30 seconds or larger. A sample time T_0 of 0.5 seconds was used for all controllers.

2.5 Minimum Variance Controller

The minimum variance controller seeks to minimize the variance of the controlled variable:

$$var[y(k)] = E\{y^2(k)\}$$
$$where\ E\{\cdot\}\ is\ the\ expected\ value\ operator$$

That is, the control is chosen based on the prediction of the output.

In this case, with the fixed rudder rate, three possible choices of rudder input exist at any sampling instant:
- move the rudder left.
- move the rudder right.
- keep the rudder at its current position.

The input is further restricted when the rudder reaches its maximum amplitude. In this case, the possible choices of rudder input are limited to decrease rudder angle or keep the rudder angle the same.

It was found early that minimizing the variance of the output alone did not produce satisfactory results. It is necessary to

18

add two terms into the criterion to be minimized:

$$I(k+1) = E\{y^2(k+1) + K[y(k+1) - y(k)]^2 + \rho u^2(k)\}$$

The second term is used to represent the velocity of the output variable and K is weighting on it, and ρ is a weighting on the control input.

After a large number of simulations were run, it was found that the weighting K had a large range of variation for different operating conditions.

Therefore a new method was found. In this method an "ideal" set-point, s(k), is added:

$$I(k+1) = E\{[y(k+1) - s(k+1)]^2 + \rho u^2(k)\}$$

Where s(k+1) is the predicted value of an idealized natural response given the previous values of the output. This method is similar to pole-placement in that a desired response is specified. The controller minimizes the variance between the desired response and the actual response.

In implementing this type of control, it is convenient to modify the difference equations (2) and (3) by multiplying them by Δ ($\Delta = (1-z^{-1})$). The result is :

$$(1-z^{-1})(1 + a_1 z^{-1} + a_2 z^{-2})\psi = b_1 z^{-1}\Delta u + b_2 z^{-1}(1-z^{-1})\phi$$

$$(1-z^{-1})(1 + a_1 z^{-1} + a_2 z^{-2})\phi = b_1 z^{-1}\Delta u + b_2 (z^{-1} - z^{-2})(1-z^{-1})\psi$$

That is, the output is now dependent on the change in u.

The control algorithm then is to:

- identify the parameters in the two difference equations
  using AML.

- compute the expected values of ψ and ϕ for the three
  possible control inputs (rudder right, rudder left, or no
  rudder movement).

- choose the rudder movement which minimizes :

$$I(k+1) = E\{ [\psi(k+1) - s_\psi(k+1)]^2 + K_r[\phi(k+1) - s_\phi(k+1)]^2 + \rho u^2(k) \}$$

The minimum variance controller was chosen because it is the
basic controller for the regulation of systems with stochastic
disturbances.

2.6 GPC Controller

The Generalized Predictive Control controller is an N step ahead
predictor. It predicts the output N steps ahead, given current
values of the inputs, outputs, and plant parameters.

In this application, two types of GPC control were evaluated.
The first is bang-bang GPC control. The cost function

$$J = [H_{N_u}\tilde{u} + \Psi_0]^T I_{mN} [H_{N_u}\tilde{u} + \Psi_0]$$

where H_{N_u} = *Predicted response of the system based on $\tilde{u}$*
         $\tilde{u}$ = *Future controls* $[\Delta u(k) \quad \Delta u(k+1) \quad \dots \quad \Delta u(k+1-N_u)]^T$
         Ψ_0 = *Predicted free response at sample k*
         N_u = *Control horizon*
         N = *Prediction horizon*

20

is calculated explicitly for the three possibilities of Δu. If
the rudder reaches its amplitude limit, there are only two
possibilities for Δu.

The control horizon used was one. The prediction horizon is
based on the slowest rise time of the system, usually the yaw
rate. A prediction horizon of 10 was used. The algorithm is
then to identify the parameters of the system using AML, predict
the output for the three possible inputs, and implement the one
which minimizes **J**.

The second type of GPC control was rate constrained GPC. Here
the control was calculated to be:

$$\tilde{u} = \left\{ \left[H_{N_U}^T H_{N_U} \right]^{-1} H_{N_U}^T \Psi_0 \right\}$$

Because the control horizon is one, the rate constraint is
implemented easily. The algorithm is check if Δu exceeds the
rudder rate, if yes then set Δu equal the rudder rate, otherwise
implement Δu calculated. Setting Δu equal to the rudder rate is
not arbitrary. It is assumed the constrained optimum lies on the
boundary of the cost function and the constraint. A prediction
horizon of 10 was also used for the rate constrained GPC.

GPC was chosen for rudder roll reduction because it is both a
good regulator and tracker. Extensive research done recently on
this type of adaptive control has shown it to be robust and
stable [9-12]. It can be extended to multivariable systems.

21

2.7 Discrete-Time Sliding Mode Control

Sliding Mode control is based on a discontinuous control function that switches when it crosses a boundary in the state space. When the states repeatedly cross this boundary and move toward the origin of the space, the system is said to be sliding. During this time the system is remarkably robust in the presence of disturbances and parameter variation. The resulting control structure is usually non-linear and results in a Variable Structure System (VSS), where the control is different in different parts of the state space. The simplest discontinuous control device is a device with two control states, e.g., a relay. For rudder roll reduction, the two control states are move the rudder right and move the rudder left.

The design procedure is to specify a nominal **A** and **B**, that is a general or average quantitative expression of the system. Solve the following matrix Ricatti equation for P :

$$P = Q + A^T P A - A^T P B R_R B^T P - P B R_R B^T P A + P B R_R B^T P B R_R B^T P$$

$$\text{where} \quad R_R = RudderRate$$
$$Q = Positive\ Definite\ Matrix$$

The sliding sub-space coefficients are then:

$$G = B^T P$$

and the control input is:

$$\Delta u = -R_R \, sign \, (\, Gx \,)$$

The preceding control input can lead to chattering, or the rapid switching of the control between two values. The fact the control input can be zero movement, besides moving right or left, and the idea of a boundary layer will be used to smooth out the chattering.

Instead of using a discontinuous surface, a small region will be constructed around the discontinuous surface. If the states are within this region, the control input used will be no change in rudder angle. In other words,

$$If \, | \, S(k) \, | \, = \, | \, Gx(k) \, | \, < \, \epsilon \quad then \quad u(k) \, = \, 0$$
$$where \, \epsilon \, is \, the \, boundary \, layer \, width.$$

Sliding Mode control was chosen because it has been used in a situation similar to rudder roll reduction of a ship, the control of transverse motions of aircraft [16]. Sliding mode control can be used with multivariable control and uses a discontinuous control input, as the fixed rudder rate is.

2.8 Pole Placement Control

The pole placement controller attempts to place the closed loop poles of the system at some arbitrary location. Given the state

23

space system:

$$x(k+1) = Ax(k) + Bu(k)$$

and assuming the input has the form:

$$u(k) = -Kx(k)$$

then the closed loop response of the system is:

$$x(k+1) = [A - BK]x(k)$$

and by setting **K**, the "natural" response of the system [**A-BK**] can be set arbitrarily. The order of the "natural" response is the same order of the original system **A**.

For rudder roll reduction, the yaw response was set with two stable exponential decay terms and the roll response was set as having the same natural frequency as, but a much larger damping ratio than, the open-loop roll response.

The control algorithm is:
  - identify the ship parameters in roll and yaw using AML.
  - calculate the gains **K** necessary to give the desired closed loop response.
  - calculate the rudder angle given the current states and the gains calculated.

Pole placement was implemented as a rudder roll reduction controller because of the explicit specification of the closed loop response. For example, the roll response is specified to keep the same natural frequency but increase the damping. The

possible problem of this controller is if the rudder rate is too slow, the rudder angle may begin to lag the control signal and start exciting the ship in roll. It is thought that if the yaw response is specified slow enough, the rudder lag problem may be avoided.

Part 3: Numerical Simulation

3.1 Numerical Model

The first attempt to obtain a numerical model involved the use of data available in the department from full scale tests performed in the summer of 1989. The data consisted of zig-zag trials of an approximately 40' double ender cabin cruiser. A regression analysis was performed to obtain the yaw and roll parameters. The results for yaw were good and made physical sense. The results for roll were not as good and, more importantly, did not make any sense physically. Therefore, a numerical model was implemented.

The numerical model used in this section of tests is based on the linear portion of Inoue's [22] manoeuvring model with additional terms for the roll motion taken from Bhattacharya [21]. The

equations are (see Appendix IV for more information):

$$(m + m_y)\, \dot{v} = \frac{1}{2}\rho LdV Y_v' v - (mu + m_x u - \frac{1}{2}\rho L^2 dV Y_r')\, r + Y_R + Y_W$$

$$(I_{zz} + J_{zz})\, \dot{r} = \frac{1}{2}\rho LdV[\, LN_v' + Y_v' x_s \,]\, v + \frac{1}{2}\rho L^2 dV[\, LN_r' + Y_r' x_s \,]\, r$$

$$+ \frac{1}{2}\rho L^2 dV N_\phi' \phi + N_R + N_W$$

$$(I_{xx} + J_{xx})\, \ddot{\phi} - m_y z_H \dot{v} = -b\dot{\phi} - g\Delta \overline{GM}\phi - \frac{1}{2}\rho LdV Y_v' z_H v$$

$$- [\, m_x u + \frac{1}{2}\rho L^2 dV Y_r' \,]\, z_H r + K_R + K_W$$

The hydrodynamic coefficients are estimated from basic ship characteristics alone. The coefficients were calculated from the data of the *Kynoc*, a 60-foot west coast drum seiner and the *Eastward Ho*, a 107-foot combination vessel that have been used in other research in the department. The coefficients were calculated for different speeds and loading conditions. From these coefficients a state space model was constructed for each of the different conditions. The particulars and speeds for the different conditions are given in the following tables.

Table 1. Kynoc Particulars

Particular	Condition 1 Half Load Full Speed	Condition 2 Half Load Half Speed	Condition 3 Full Load Full Speed	Condition 4 Full Load Half Speed
L_{wl} (m)	17.25	17.25	17.4	17.4
B_{wl} (m)	6.1	6.1	6.1	6.1
T_{mean} (m)	2.53	2.53	2.82	2.82
τ	1.24	1.24	1.41	1.41
Δ (tonnes)	116.5	116.5	141	141
C_b	0.43	0.43	0.46	.46
L/B	2.83	2.83	2.85	2.85
LCG (m)	-0.608	-0.608	-0.851	-0.851
VCG (m)	2.22	2.22	2.13	2.13
GM (m)	0.735	0.735	0.546	0.546
Speed (kts)	11	8	11	8

Table 2. Eastward Ho Particulars.

Particular	Condition 1 Half Load Full Speed	Condition 2 Half Load Half Speed	Condition 3 Full Load Full Speed	Condition 4 Full Load Half Speed
L_{wl} (m)	30.5	30.5	30.8	30.8
B_{wl} (m)	8.74	8.74	8.74	8.74
T_{mean} (m)	3.45	3.45	4.04	4.04
τ	0.835	0.835	1.073	1.073
Δ (tonnes)	445	445	572	572
C_b	0.472	0.472	0.514	0.514
L/B	3.49	3.49	3.52	3.52
LCG (m)	-1.405	-1.405	-1.893	-1.893
VCG (m)	3.28	3.28	3.38	3.38
GM (m)	1.161	1.161	1.268	1.268
Speed (kts)	13	10	13	9

The matrices were discretized using a zero order hold with a sampling period of 0.5s (See for example Ogata [18]).

The rudder motion has two restrictions -amplitude and rate. The amplitude is limited to ±40 degrees. The swing rate of the rudder has a maximum of 5 degrees per second. If the demanded rudder angle is within the amplitude limitations, and the difference between the previous rudder angle and the demanded rudder angle is less than or equal to the swing rate multiplied by the control cycle time, the demanded rudder angle is implemented. Otherwise, the rudder angle implemented is the closest value to the demanded angle that does not violate the two restrictions.

For the irregular wave disturbances used in some of the tests, digital filter approximations were constructed (see Appendix V). These approximations were based on excitation spectra calculated using the Bretschneider Spectrum. The approximations were matched to the spectra for shape qualitatively and for area under the curve quantitatively. Examples of sway and yaw excitation are contained in Figures 3 and 4. Figure 5 shows an example of wave slope. Roll Excitation was simply $\Delta GM \times$ wave slope.
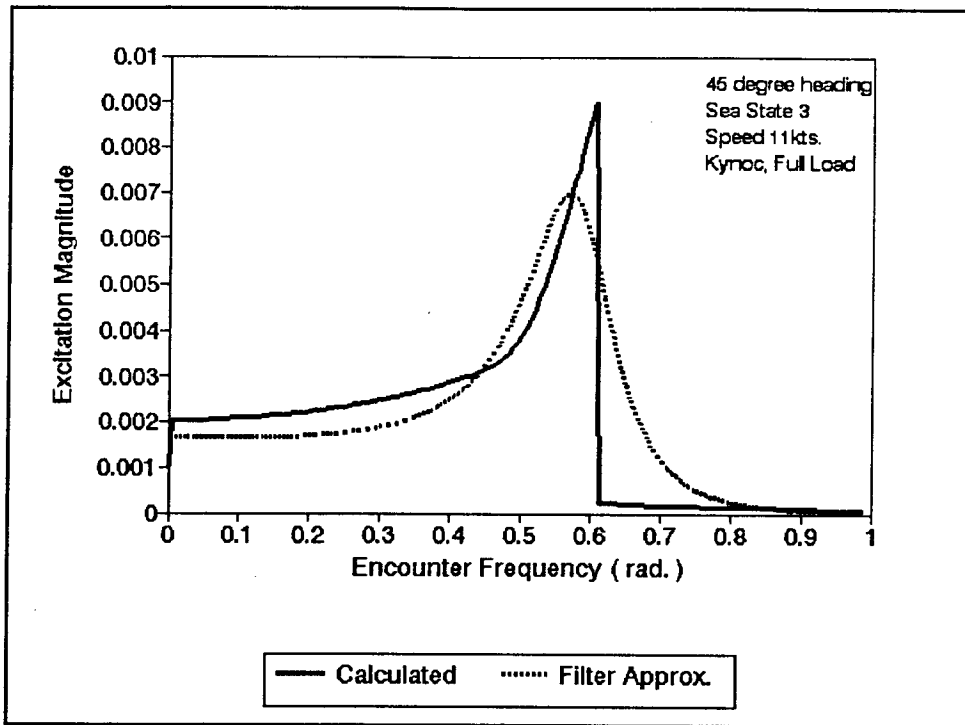
Figure 3. Sway Excitation Spectrum
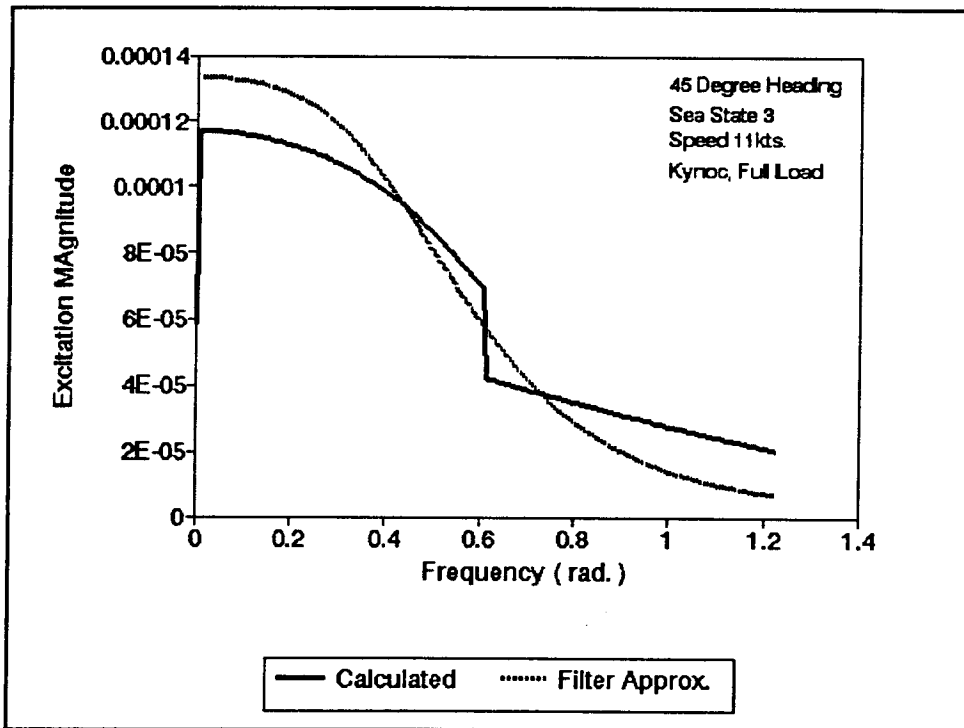
Figure 4. Yaw Excitation Spectrum
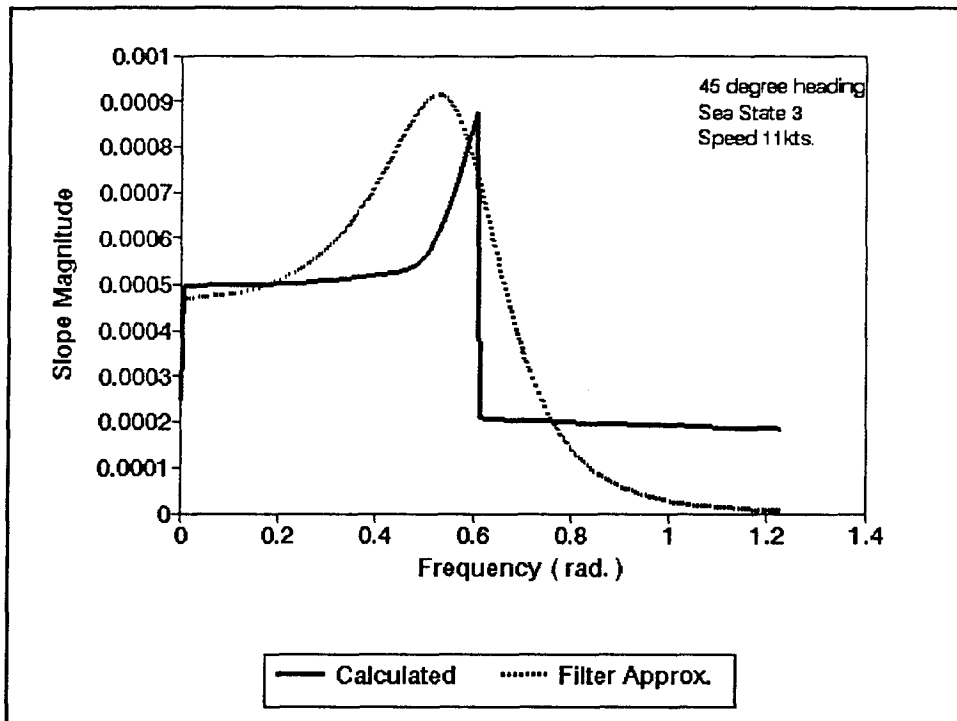
Figure 5. Slope Spectrum

In these tests, the state equations were:

$$x(k{+}1) = Ax(k) + Bu(k) + Kw(k)$$

where w(k) is a vector of the values from the three excitation filters.

3.2 Controller Parameters

The controller parameters that can be adjusted were set for all tests. The test used to specify these parameters consisted of giving the vessel an initial yaw offset of 10° so that the controller had to move the vessel to a zero yaw angle as quickly

31

and smoothly as possible.

For the controllers under evaluation, simple autopilots were constructed to compare the amount of roll reduction produced.

The parameters for the autopilots were as follows:

- PID Controllers. The parameters of the PID controller for the *Kynoc* were $K=-1$,$T_D=0.5$, and $T_I=30$. The PID parameters for the *Eastward Ho* were $K=-1$,$T_D=1.0$, and $T_I=45$.

- Minimum Variance Controllers. The ideal roll response was characterized by the equation $1 - 1.59z^{-1} + 0.764z^{-2}$, corresponding to a natural frequency of 7 seconds and a damping ratio of 0.3. The ideal yaw response for the *Kynoc* had a characteristic equation of $1 - 1.6z^{-1} + 0.6399z^{-2}$. The characteristic equation of the ideal yaw response for the *Eastward Ho* was $1 - 1.8z^{-1} + 0.8099z^{-2}$. K_r was set to 1 for both vessels. The simple autopilots used the same ideal yaw responses for the respective vessels. The *Kynoc*'s autopilot used $\rho=0.0003$, the *Eastward Ho* used $\rho=0.00005$.

- GPC Controllers. For both vessels, the roll reduction autopilots used $N=10$. The simple autopilots for both vessels used $N=11$.

- VSS Controllers. The switching surfaces for the roll

reduction autopilot, the simple autopilot, and the 15°/s
rudder rate roll reduction autopilot were the same for both
boats. The nominal system used for rudder roll reduction
was:

$$A=\begin{bmatrix} 1.8 & -0.8 & 0 & 0 & 0.03 \\ 1 & 0 & 0 & 0 & 0 \\ -0.3 & 0.3 & 1.7624 & -0.9561 & 0.01 \\ 0 & 0 & 1 & 0 & 0 \\ 0 & 0 & 0 & 0 & 1 \end{bmatrix} \quad B=\begin{bmatrix} 0.03 \\ 0 \\ 0.01 \\ 0 \\ 1 \end{bmatrix}$$

This system has a yaw rate time constant of 2.24 seconds, a
roll natural period of 7 seconds, and a roll damping ratio
of 0.05. The roll reduction autopilot's switching surface
was G=[43.06 −38.32 16.69 −0.839 4.6215]. The boundary layer
used for the *Kynoc* was ϵ=0.05; the boundary layer for the
Eastward Ho was ϵ=0.025. The nominal system used for the
simple autopilot was:

$$A=\begin{bmatrix} 0 & 1 & 0 \\ 0 & 0 & 1 \\ 0.8 & -2.6 & 2.8 \end{bmatrix} \quad B=\begin{bmatrix} 0 \\ 0 \\ 0.017 \end{bmatrix}$$

The simple autopilot's switching surface was G=[107.8961
−254.926 150.573]. The boundary layers used were 0.09 for
the *Kynoc* and 0.04 for the *Eastward Ho*. The 15°/s roll
reduction autopilot had a switching surface of G=[14.24
−12.67 5.56 −0.3188 1.536]. The boundary layers were 0.06
for the *Kynoc* and 0.03 for the *Eastward Ho*.

- Pole Placement Controllers. The roll poles, which were
the same for both boats, were placed at 0.798±0.363i. These

locations correspond to a natural frequency of 7 seconds and a damping ratio of 0.3. The *Kynoc*'s yaw poles were placed at z=0.79 and z=0.81. The *Eastward Ho*'s yaw poles were places at z=0.89 and z=0.91.

3.3 Tests

After each controller was chosen, designed, and parameters set, the following tests were simulated using the numerical model:

1. A 15 degree course offset. This offset is 50% larger than the design offset of 10°. The half load full speed ship was used for this test.

2. A yaw velocity impulse of 5.7°/s. This test is the base case for the following four tests.

3. Change in speed. The speed was decreased to half speed, which decreases the effectiveness of the rudder and thereby increases the settling time.

4. Change in displacement. The full-load, full-speed condition was used for this test. This condition increases the yaw rate decay time and thereby increases the settling time.

5. Change in speed and displacement. This test uses the full-load, half-speed condition. In this test the controller

response to both a change in speed and displacement was
measured.

6. Rudder servo slows by 20%. The purpose of this test was to
   see how well the controller works when the actuator's
   performance has been degraded slightly. This situation
   could occur due to poor maintenance (e.g., hydraulic fluid
   leakage or simple wear).

7. A constant yaw moment. This test simulates effects such as
   prop walk, steady wind and current effects that would
   produce a constant yaw moment. The half-load, full-speed
   condition was used for this test.

8. Irregular beam (90°) seas. This heading should produce the
   worst roll motions. The full-load, half-speed case was used
   because this loading condition has the lowest roll
   stability. The modal frequency of the sea state was set
   equal to the roll natural frequency and the significant wave
   height was one hundredth of the length of wave with a period
   equal the roll period ($H_{\nmsp}=0.01gT_{\phi}^{2}/(2\pi)$ and $T_m=T_{\phi}$) .

9. 45 degree quartering seas. Quartering seas produce the most
   excitation for roll and yaw combined; thus three quartering
   seas tests were run. The full-load, full-speed condition was
   used for this test. Sea State 3 for the North Pacific was
   used for the modal frequency and significant wave height
   ($H_{\nmsp}=0.88m$ and $T_m=7.5s$).

10. 60 degree quartering seas. The half-load, full-speed condition was used in this test. Sea State 3 for the North Pacific was used for the modal frequency and significant wave height.

11. 30 degree quartering seas. The half-load, half-speed condition was used in this test. Sea State 4 for the North Pacific was used for the modal frequency and significant wave height ($H_{\frac{1}{3}}$=1.88m and T_m=8.8s) .

Different load and speed conditions were used in the irregular sea tests to obtain a better idea of the range of behaviour. The irregular sea cases (tests 8-11) were then rerun for both vessels using a rudder rate of 15°/s. Only the four better roll reduction autopilots, the VSS, the pole placement, the minimum variance, and the rate constrained GPC, as well as the PID and the pole placement autopilots were run.

3.4 Results

The results are tabulated in Appendix VI. The impulse responses from the *Kynoc* of the PID autopilot, the VSS roll reduction and simple autopilots, and the pole placement roll reduction and simple autopilots are shown in Figures 6 to 10. These figures are examples of the deterministic tests and show the effect of adding rudder roll reduction .
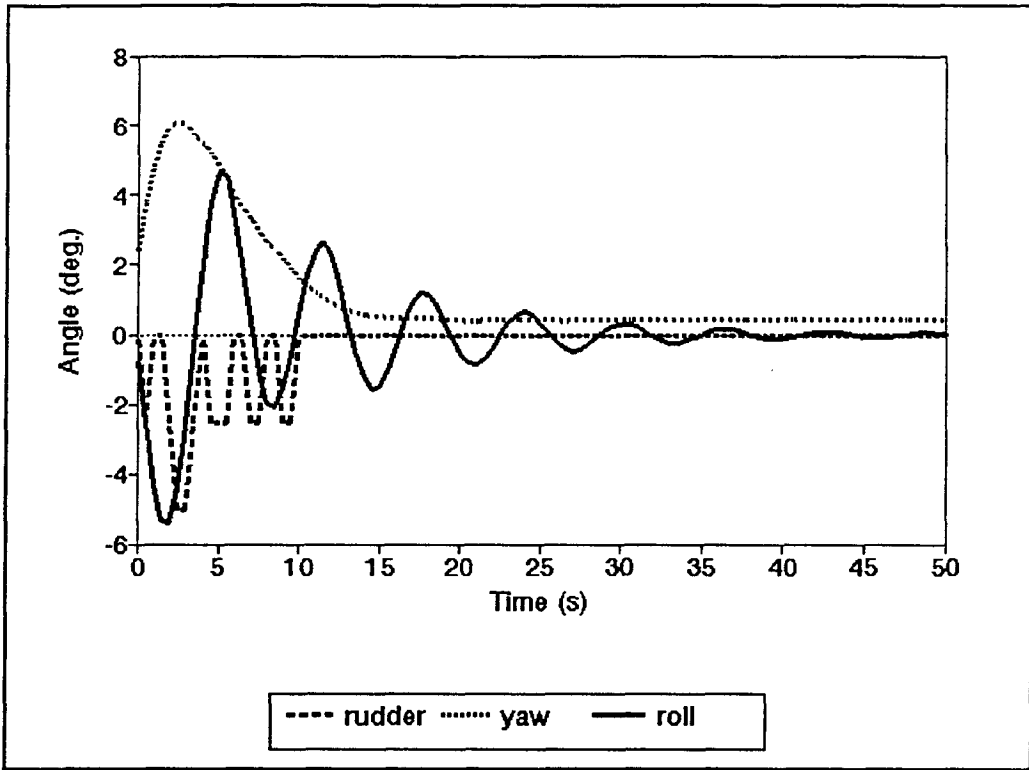
Figure 6. VSS Impulse Response for *Kynoc*
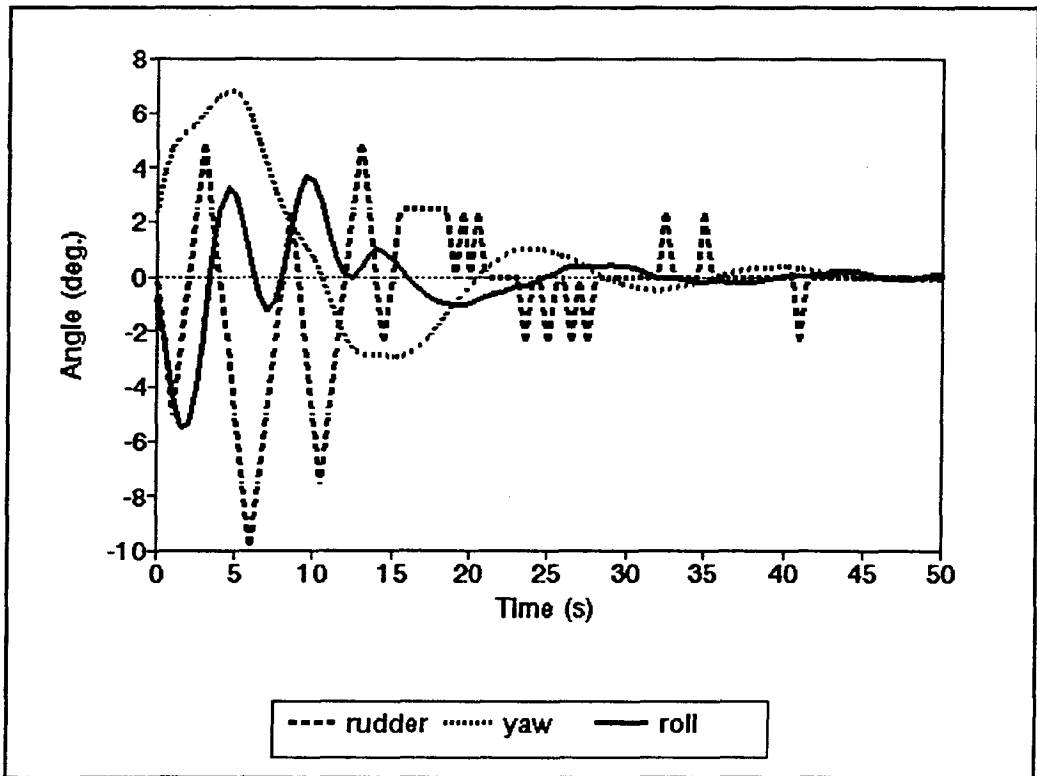
Figure 7. VSS Roll Reduction Impulse Response for *Kynoc*

37
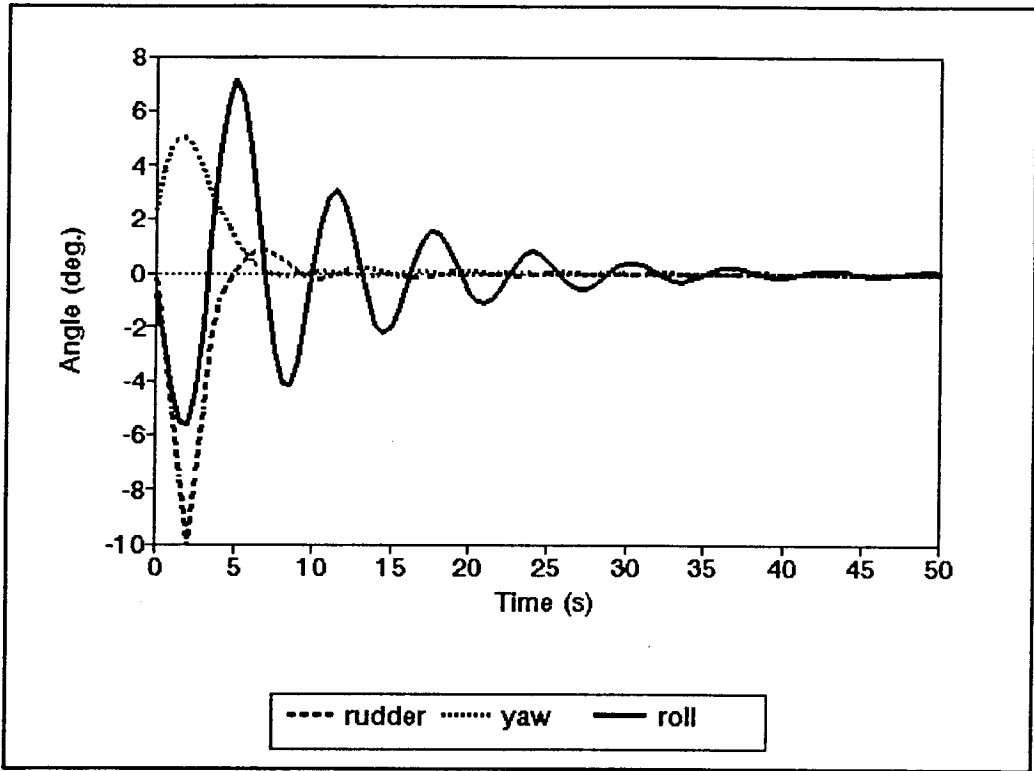
Figure 8. Pole Placement Impulse Response for *Kynoc*
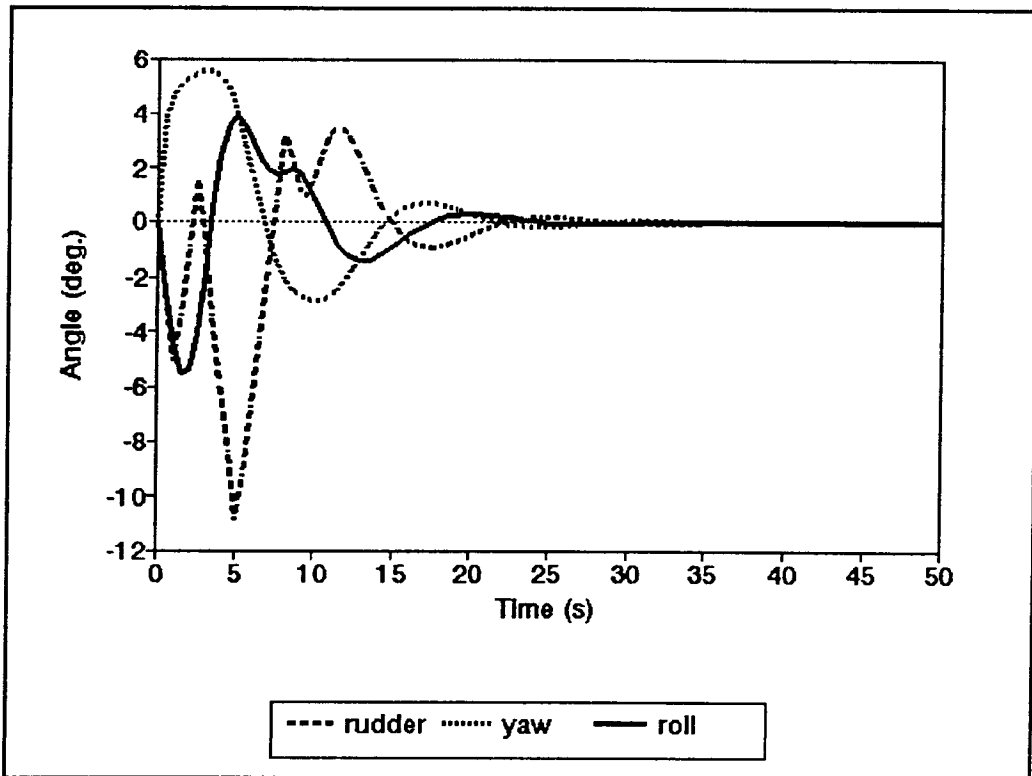
Figure 9. Pole Placement Rudder Roll Reduction Impulse Response for *Kynoc*
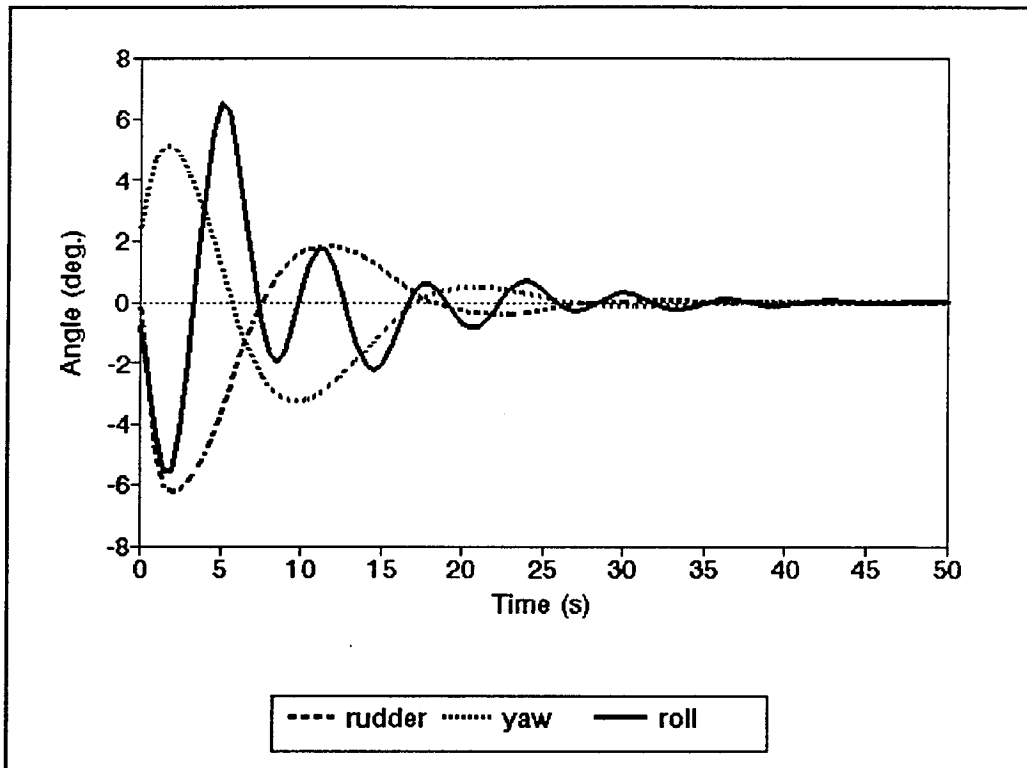
Figure 10. PID Impulse Response for *Kynoc*

The more relevant tests are the irregular sea tests because in these tests both roll and yaw are excited and because these tests typify the conditions where a ship's operator desires roll reduction. For convenience, the results from the irregular sea tests for controllers with a 5°/s rudder rate are presented in Figures 11 to 18. The figures show the RMS roll and yaw angles, smaller values being better for each. The increase in roll reduction for the controllers tested with a 15°/s rudder rate are also provided in Figures 19 to 22. All tests were run for a time of 10 minutes. An angular value of 20 degrees for any of yaw, roll, or rudder angle was considered to exceed the valid range of the numerical model.

In general, the simple autopilots had good results, often better

than their roll reduction counterparts.

The adaptive controllers on the *Eastward Ho* tests did not do well, often exceeding the valid yaw range of the numerical model. The constant yaw moment test on both vessels caused problems with many of the controllers.

One unusual result was that better course keeping resulted in better roll response. It was expected there would be a trade-off of worse yaw response for better roll response. The other unusual result was that the increase in the rudder rate to fifteen degrees per second did not improve the roll results for any of the controllers. The controller helped most by the increased rudder rate was the pole placement roll reduction controller; however, the increase in performance was not consistent over all the tests.

The results are summarized for each controller as follows:

- The PID autopilot did surprisingly well, as it was expected to have problems with rudder phase lag in the more extreme irregular seas. The actuated rudder angle always matched the command rudder angle from controller.

- The minimum variance autopilot had excellent course keeping in almost every test.

- The VSS autopilot did extremely well, its course keeping was phenomenal.

- The pole placement autopilot had excellent results; however, the actuated rudder angle did not always match the command rudder angle from the controller.

- Both GPC autopilots had fair results, but better performance was expected.

- All the roll reduction autopilots did poorly. The best roll reduction controller is the VSS roll reduction controller which outperforms the PID controller in six out of eight cases. The next best controller is the pole placement roll reduction autopilot, which is better than the PID controller four out of eight times.
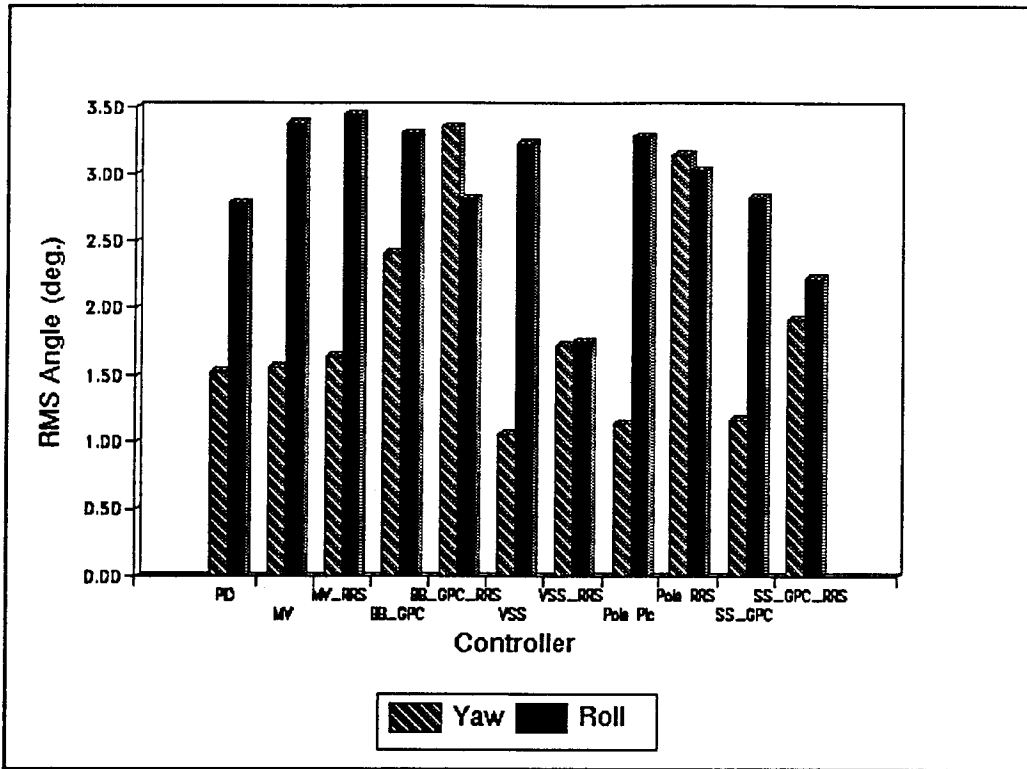
Figure 11. Kynoc 90° Seas
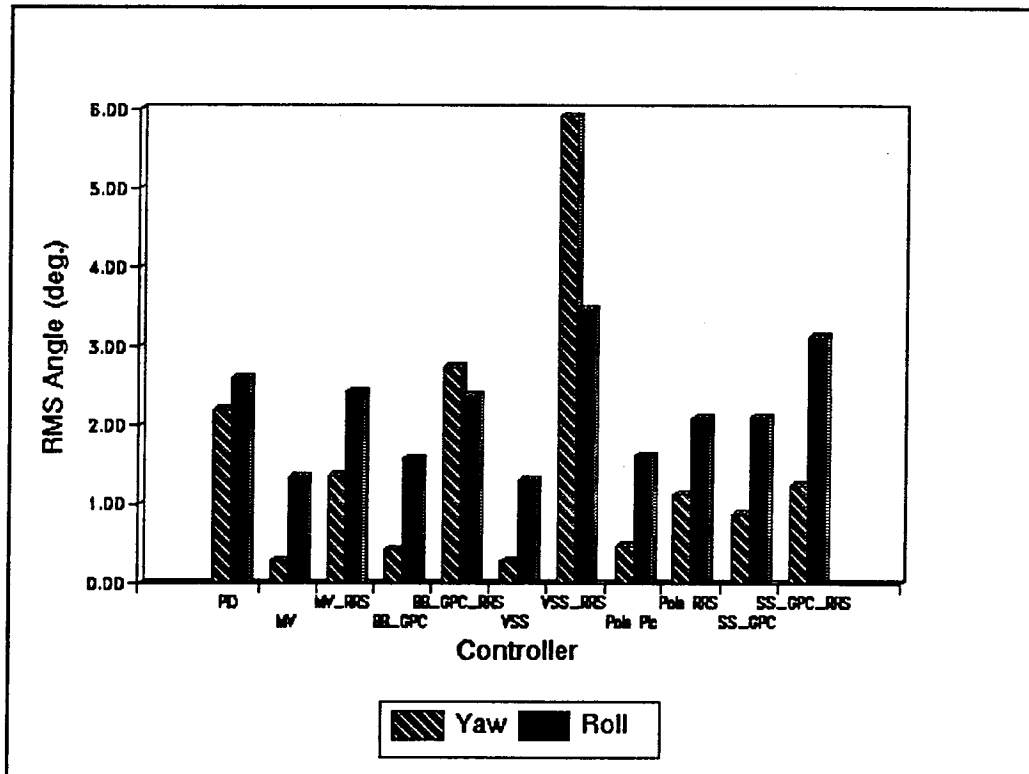
Figure 12. Kynoc 45° Seas

42
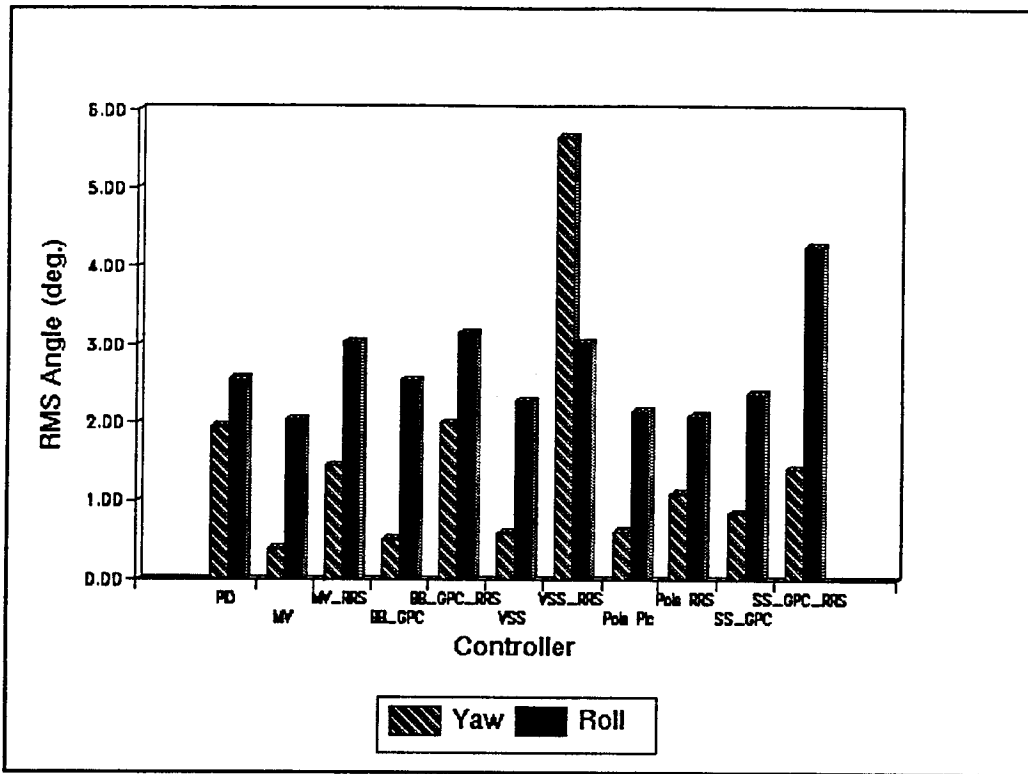
Figure 13. Kynoc 60° Seas
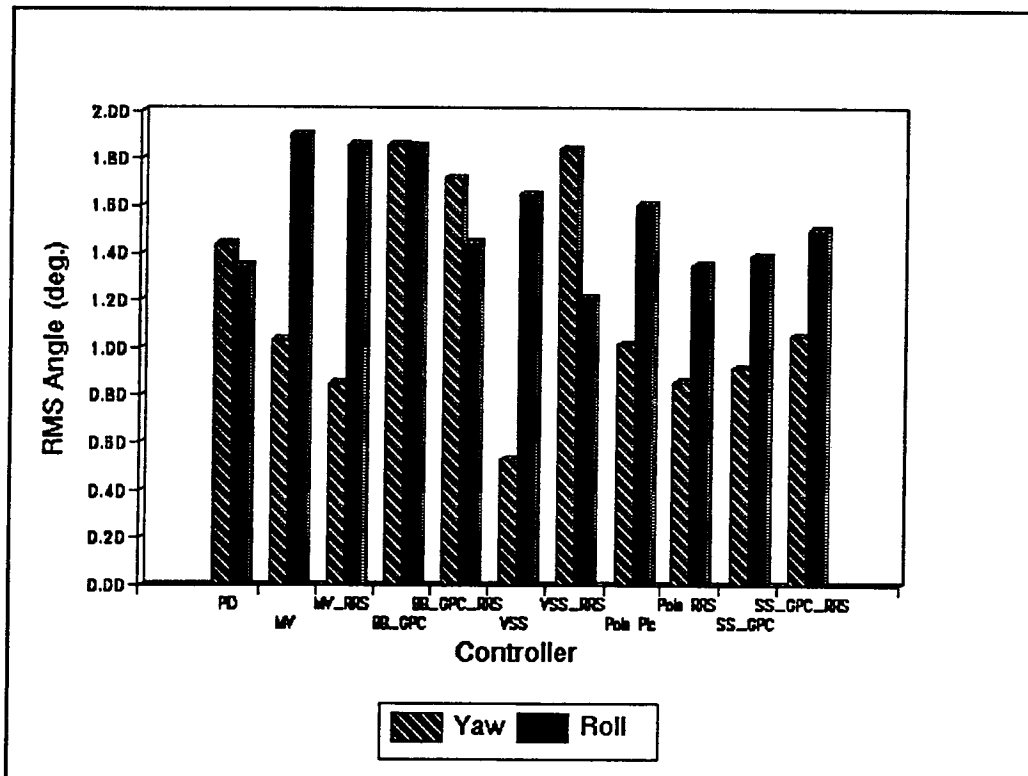
Figure 14. Kynoc 30° Seas

43
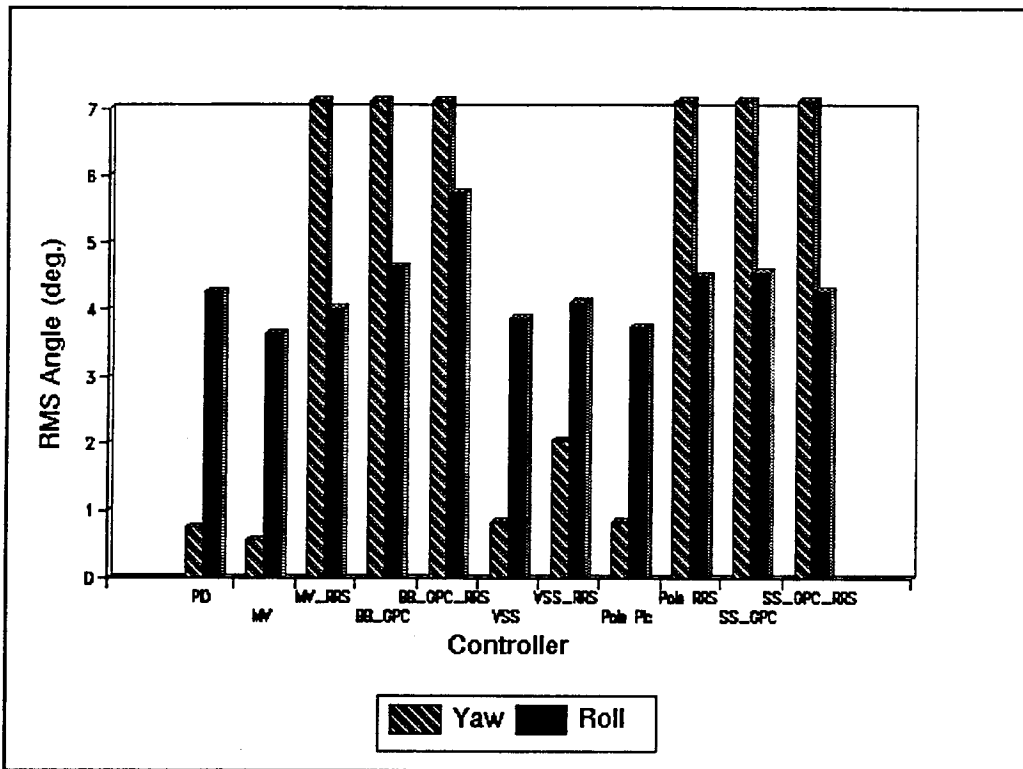
Figure 15. Eastward Ho 90° Seas
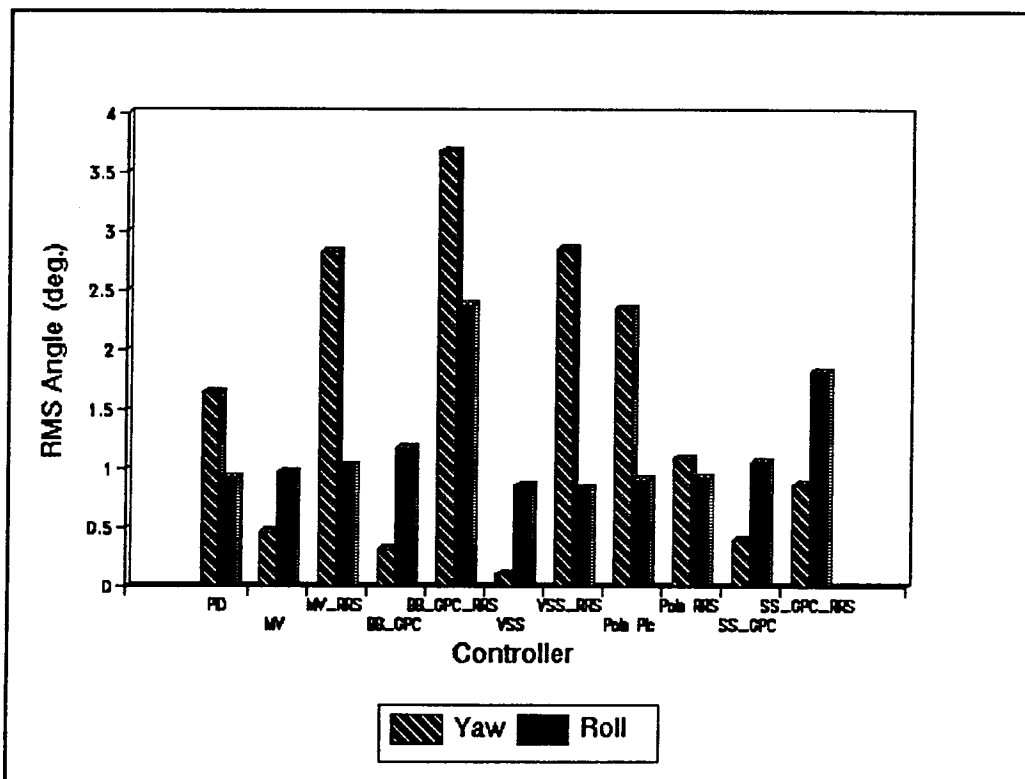
Figure 16. Eastward Ho 45° Seas
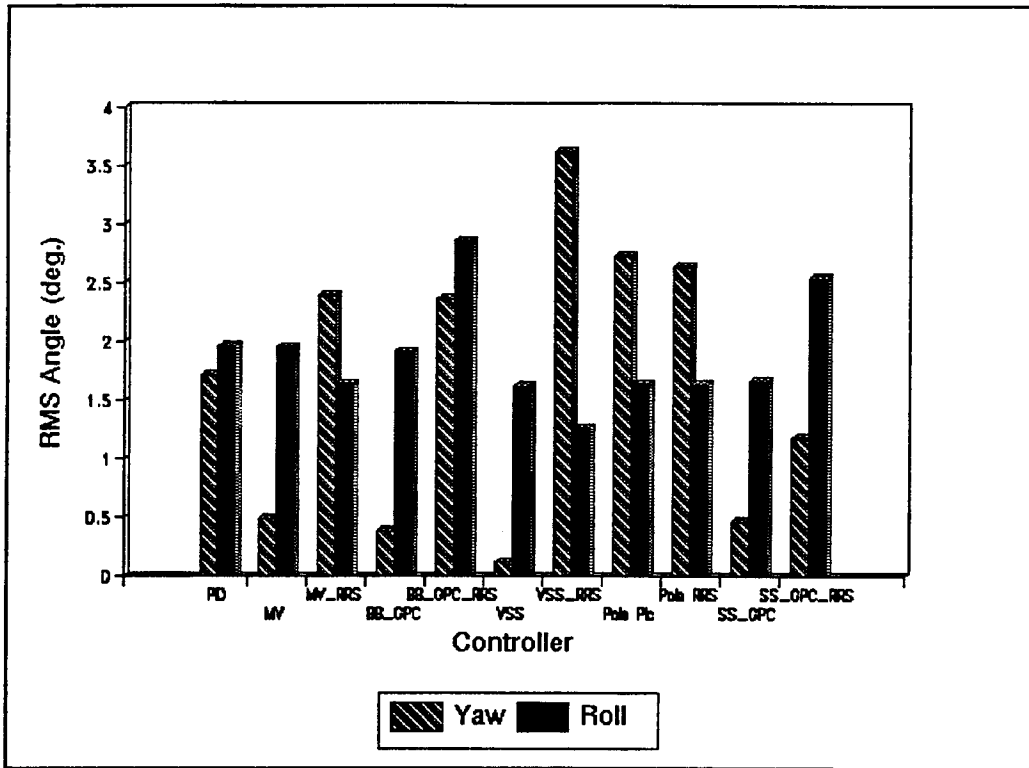
Figure 17. Eastward Ho 60° Seas
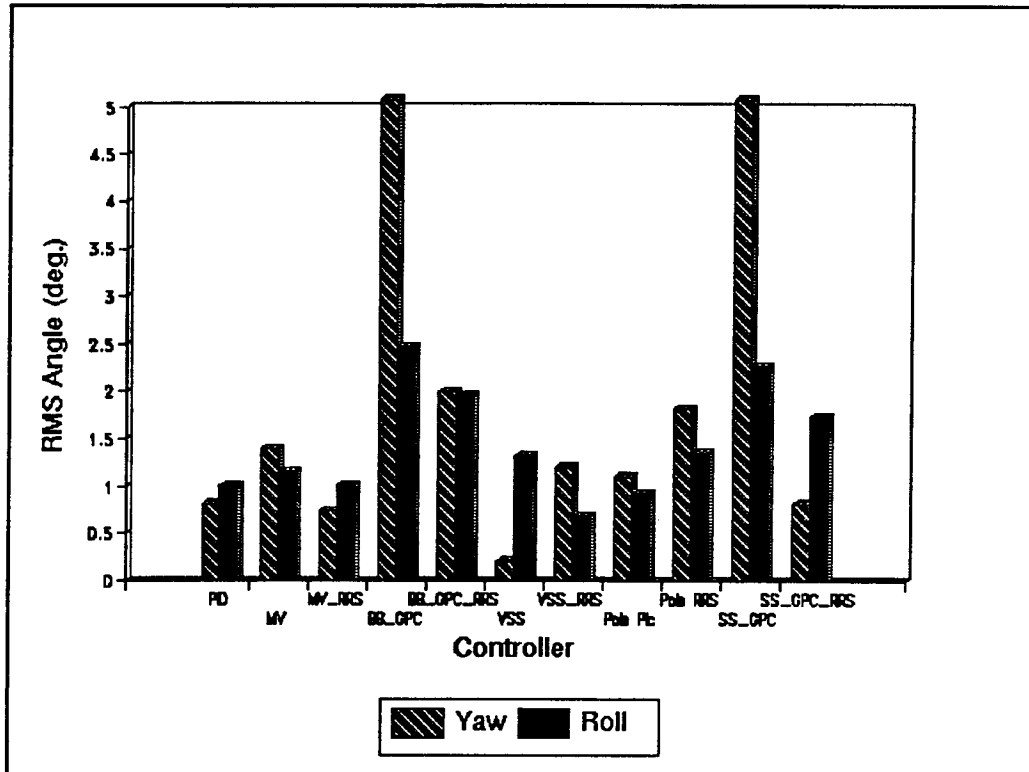
Figure 18. Eastward Ho 30° Seas
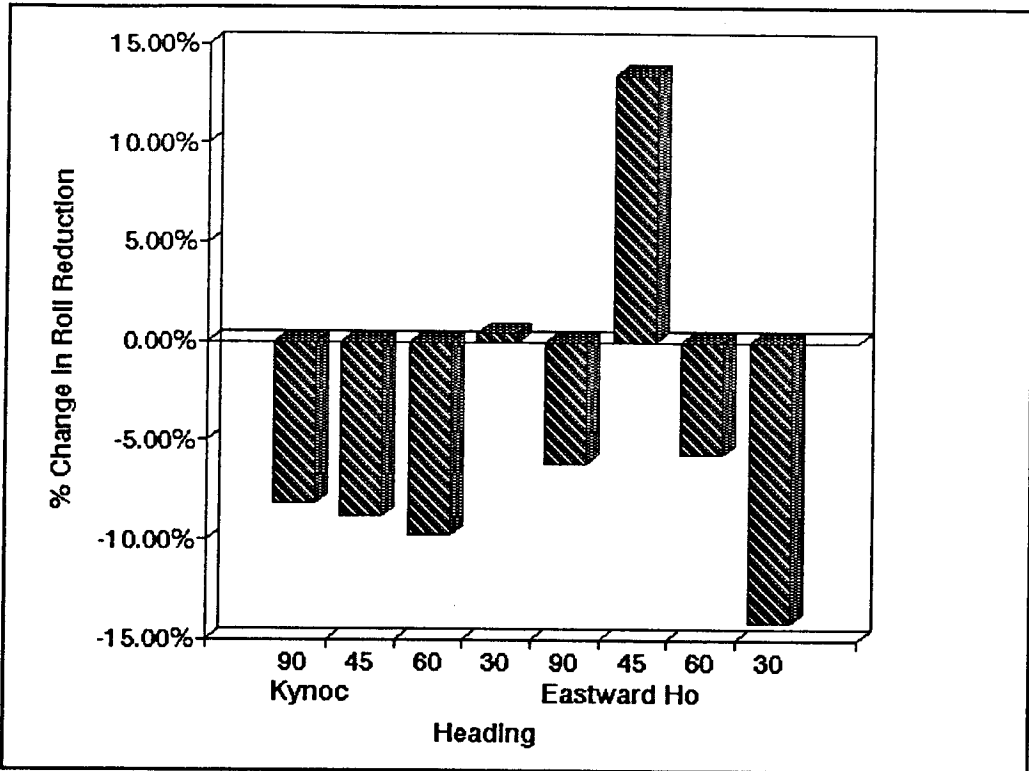
Figure 19. VSS Roll Reduction Improvement 15°/s Rudder Rate
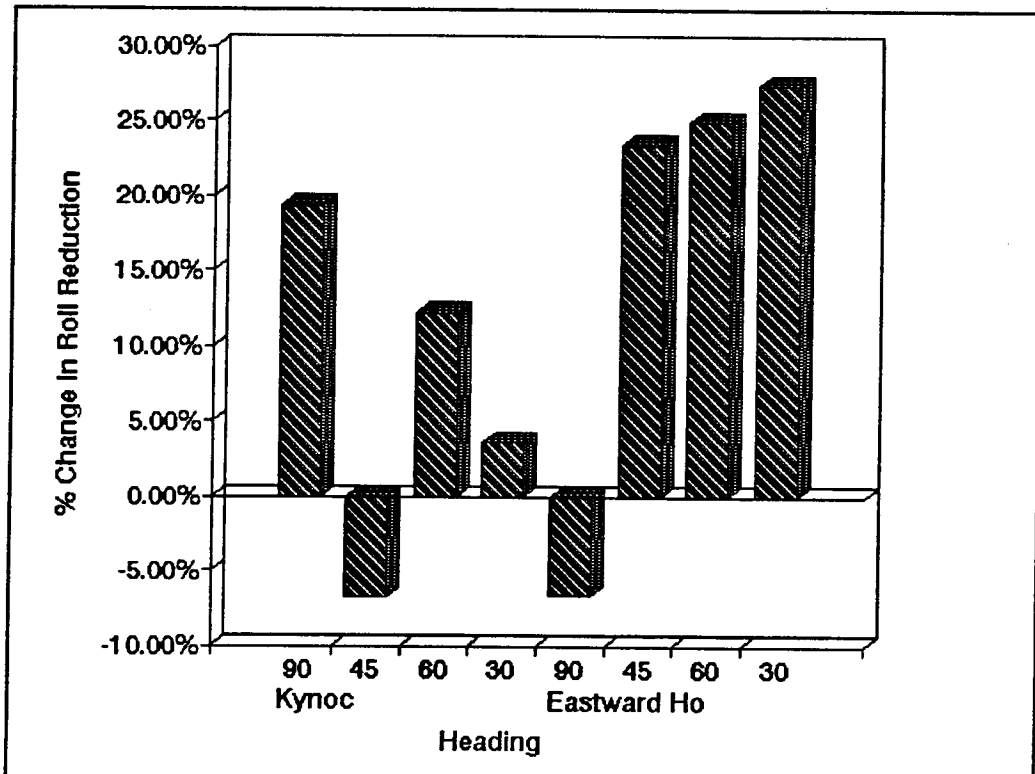
Figure 20. Pole_RR Roll Reduction Improvement 15°/s Rudder Rate
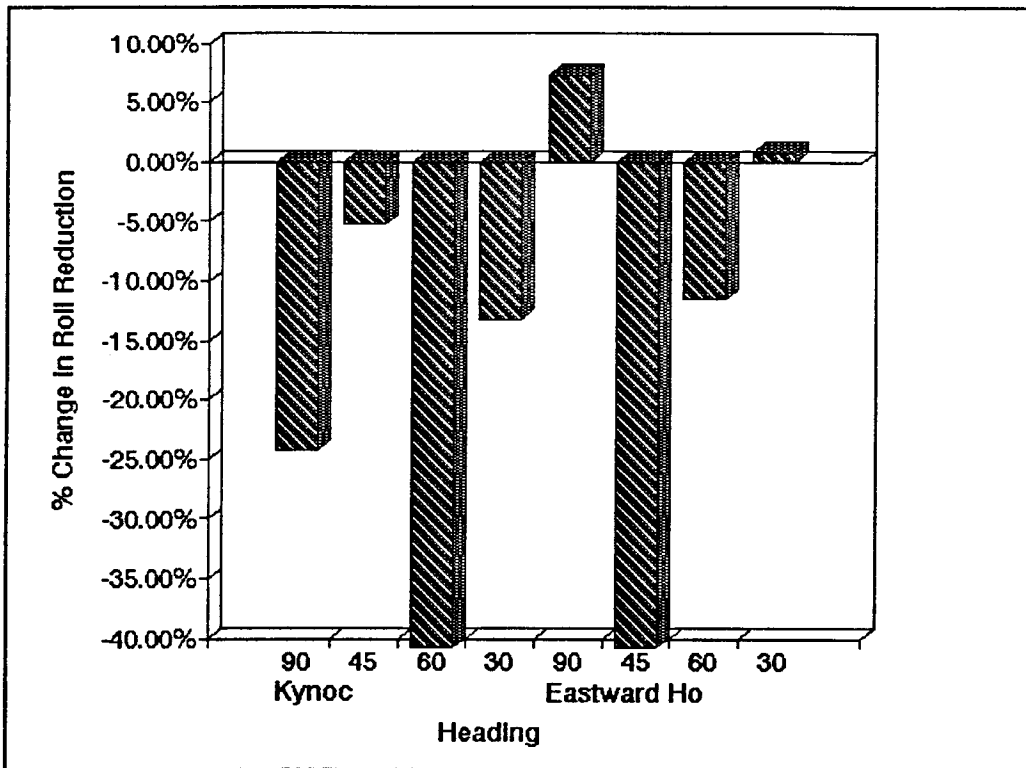
Figure 21. MV_RR Roll Reduction Improvement 15°/s Rudder Rate
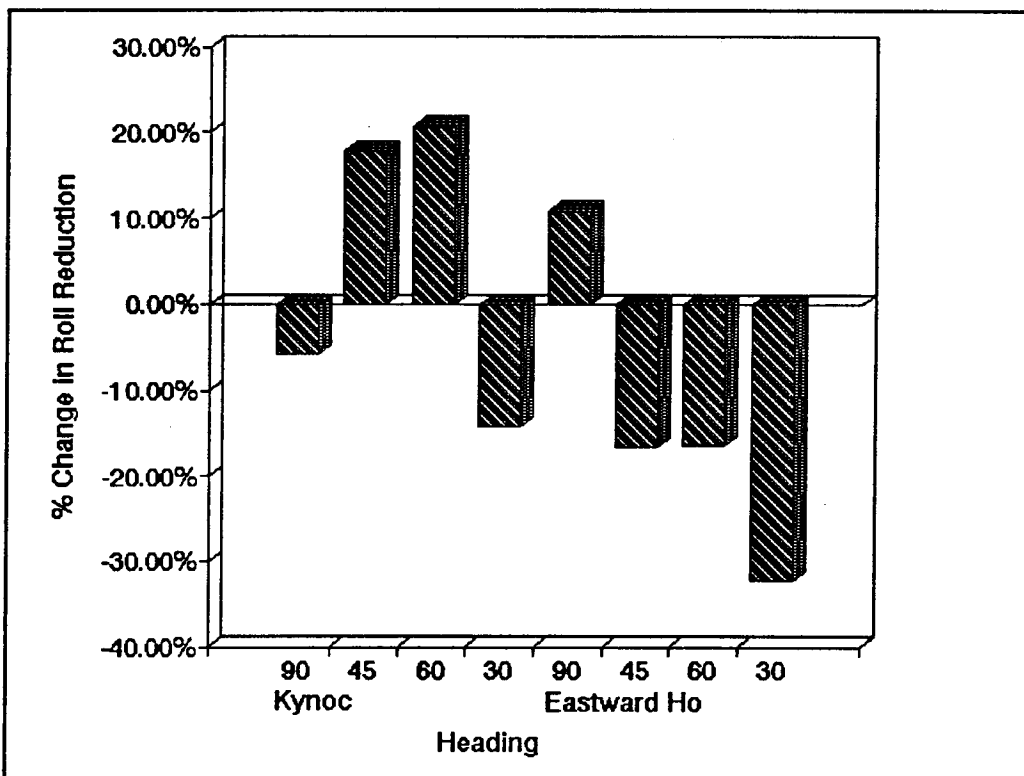
Figure 22. SS_GPC_RR Roll Reduction Improvement 15°/s Rudder Rate

3.4 Evaluation of Roll Reduction

Based on the numerical simulations, rudder roll reduction does not work well enough for commercial implementation on fishing boats. None of the roll reduction controllers reduced the roll motion below that of the PID controller in every irregular sea case.

The result from the numerical simulations that rudder roll reduction does not work is suspect for several reasons. The first reason is that some of the controllers exceeded the valid yaw range of the numerical model in the *Eastward Ho* tests. The reason for these results was found by comparing heeling moment produced by the rudder to the wave induced roll moment. For a wave induced roll moment produced by a wave with a period equal to the *Eastward Ho*'s natural roll period and a wave height of one hundredth the wave length, the rudder angle necessary for the heeling moment to counteract the wave moment is 51°. The resulting heading angle is 60°. Both these values are well outside the numerical model's range. In comparison, the *Kynoc*'s rudder angle is 15° and the yaw angle is 19° for a wave with the *Kynoc*'s natural roll period. The reason for the large difference between the two boats is the *Kynoc* has a more effective rudder.

The second reason comes from comparing the results in this study to previous results in literature [3,5,8], where roll reduction was reported successful. To compare the same qualities on

Table 3. Dimensionless Quantities

Dimension less quantity	GM_T/L	z_R/L	A_R/L^2	F_n	T_ψ/T_ϕ	$1/(\delta \times T_\phi)$
Kynoc	0.037	0.126	0.0046	0.32 – 0.435	0.21	0.028
Eastward Ho	0.040	0.077	0.0027	0.26 – 0.39	0.23	0.029
USCGC Jarvis[5]	0.0096	0.037	0.0015	0.21 – 0.24	1.37	0.02
Amerongen[3]					0.17	0.014
Kallstrom[6]	0.0026	0.031	0.0012	0.17	1.52	0.0054

different ships, the technique of dimensional analysis was used. The dimensionless quantities are presented in Table 3. The three quantities vertical distance to rudder centre of effort to length, total rudder area to length squared, and Froude Number (z_R/L, A_R/L^2, and F_n) are measures of how effective the rudder is in roll and the two boats in this study would appear to have more effective rudders. The ratio of yaw-rate decay-time to roll natural period (T_ψ/T_ϕ) for the *Kynoc* and *Eastward Ho* are not any better or worse than the vessels used in previous studies. The rudder rate to roll period fraction indicates that the boats in this study have slower rudder rates for their given roll periods; however, the rudder rates are not much slower than the USCGC Jarvis's rudder rate and the *Eastward Ho*, which has a slightly faster rudder, had poorer results than the *Kynoc*.

The third reason is the result that better course keeping gives better roll response. Intuitively, this result does not seem correct because there should be some trade-off between course keeping and roll reduction. Reasons for this result are unknown

at this time.

The last reason to suspect the result from the numerical model tests is that increasing the rudder rate did not improve the roll response. Previous results [2,3,5] indicate that increasing the rudder rate always increases the roll response and intuitively, improving the actuator should improve the system response when system improvement is possible. Reasons for the lack of improvement are unknown at this time.

The identification algorithm, used in the adaptive controllers, worked well (see Figures 23 and 24). The yaw parameter a_{2y} was typically slightly higher than expected, possibly due to the presence of sway motion.
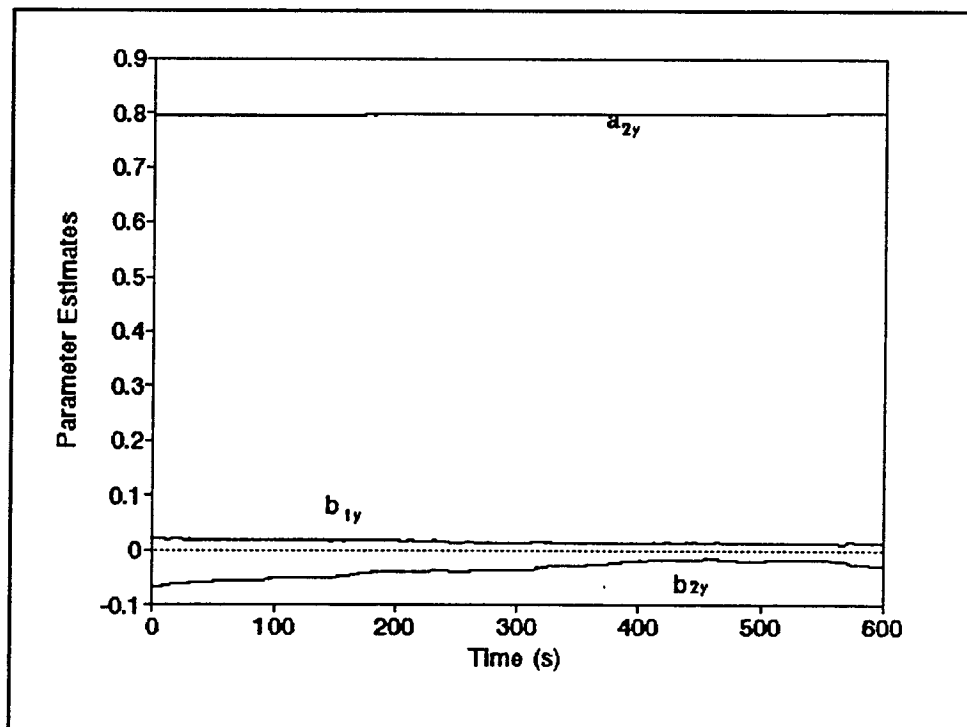
Figure 23. Example of yaw parameter identification (random sea test - Eastward Ho)
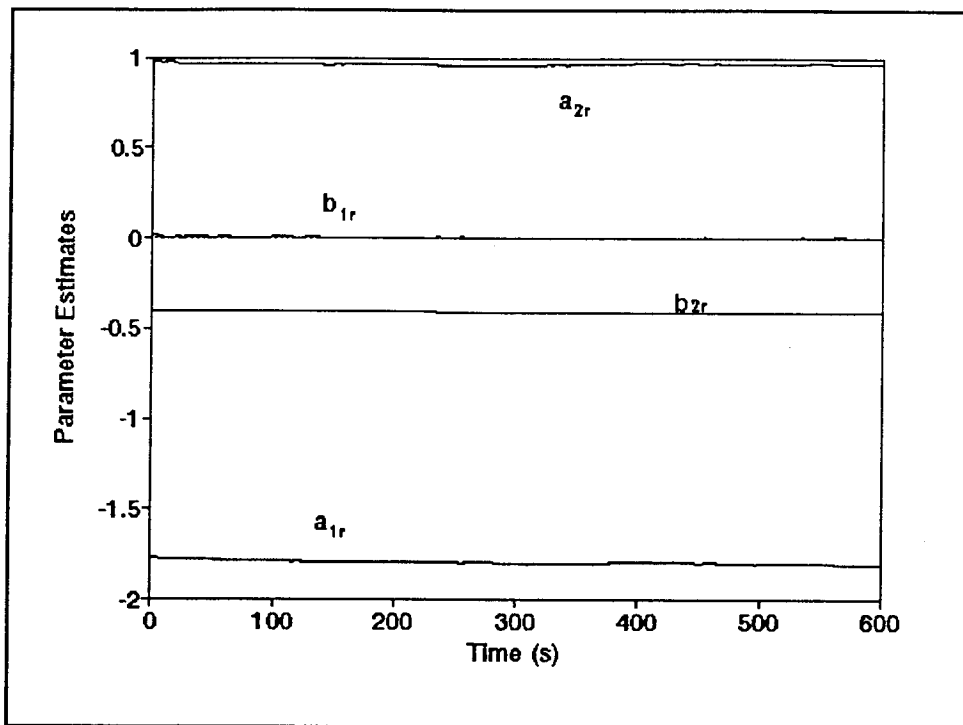
Figure 24 Sample Roll Identification (Random Sea CAse - Eastward Ho)

The poor results with the adaptive controllers were first thought to be from the adaptive algorithm because at the same time into the simulation when the yaw results started to exceed the model's range, the yaw parameter a_{2y} would rapidly change to a new value (see Figure 25). A sensitivity experiment was performed using the minimum variance roll reduction autopilot. The controller parameter K_r was reduced, in effect reducing the importance of roll reduction, and the results compared. When K_r was small enough the numerical model did not exceed its range of validity and the a_{2y} parameter did not have a rapid change (as in Figure 23). Therefore, from this experiment and the comparison of heeling moment to wave-induced roll moment, the problems with the

51

adaptive controllers are either from the controller algorithms or the numerical model and not from the adaptive algorithm or the process model used in the adaptive algorithm.
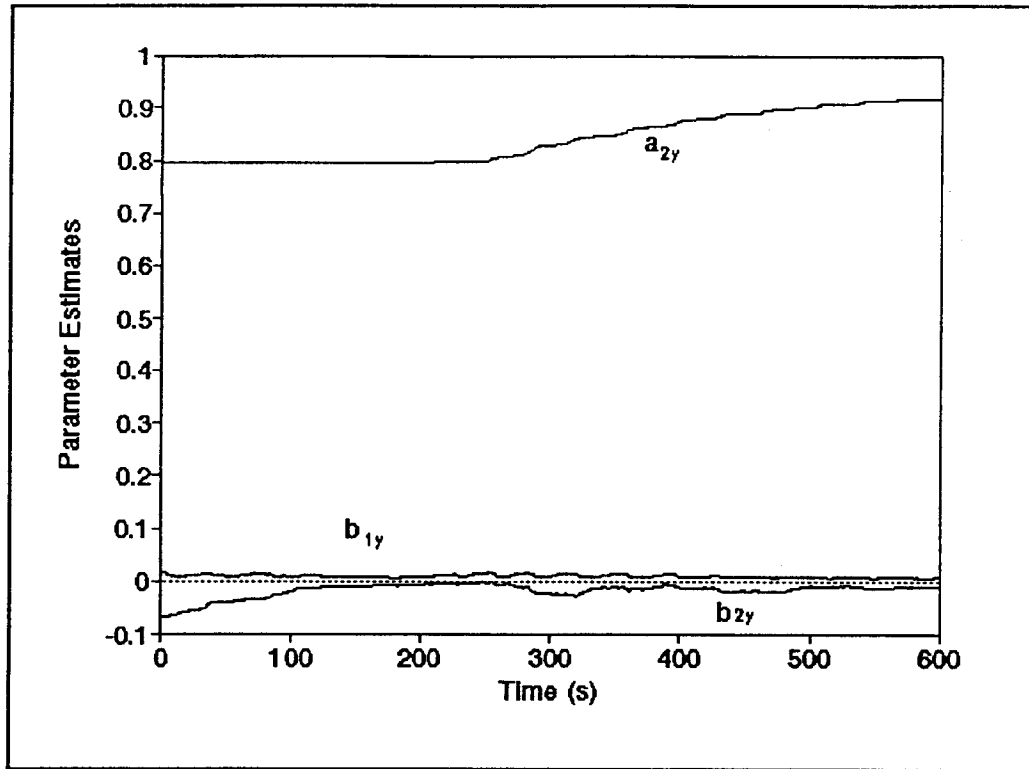
Figure 25 Yaw Parameter Estimates

The results for the VSS, the minimum variance, and the pole placement autopilots are very good, not just because of their good yaw response, but because of the form of the algorithms. These controllers have just one "tuning knob", compared to the PID controller which has three, making it easier for the ship's operator to adjust the autopilot. The minimum variance and pole placement would appear to have more than one parameter to adjust; however, the pole locations could be chosen by the controller based on the identification results, most likely the b_{1y} parameter because it shows how effective the rudder is and therefore how quickly the boat can respond.

A physical model that had been used for other self-propelled model tests was prepared for autopilot testing. The model is a 15:1 scale model of the *Eastward Ho*, a 107' steel combination vessel. The principle particulars of the model are given in the following table.

Table 4. Model Particulars.

Particular	
Length (m)	1.805
Beam (m)	0.54
Depth (m)	0.35
Draft (m)	0.22
C_b	0.5
Δ(kg)	102

Preparations for the tests included re-surfacing the outer hull of the model with a fabric composite, splining the outer hull and installing a new power bus. Two 12V 24Ah batteries and one 12V 7Ah battery were installed for power. One of the 24Ah batteries was replaces with a 31Ah battery after the old battery became damaged. A choke and capacitor were installed as power conditioners for the existing motor control unit and a capacitor was installed as a power conditioner for the rudder servomotor, respectively.

4.1 Yaw Sensor

A yaw sensor is necessary for measuring the model's direction. The first sensor installed for measuring yaw angle was a International Navigation INI-100 Digital Heading Sensor. This device is a fluxgate magnetometer, or a solid state compass. After many trials with poor results, it was discovered that there was too much distortion of the earth's magnetic field within the towing tank building.

A directional gyroscope, an Aviation Instrument Manufacturing Co. 205-2A, was then installed. This instrument is connected to a modified Wagner SEAutopilot Generation 2 autopilot to resolve the synchronous output of the gyroscope to a dc signal for the telemetry system.

4.2 Roll Sensor

The other sensor necessary in a roll reduction system is one to measure roll angle; therefore, a Humphrey VG24-0825-1 vertical gyroscope was installed. This gyroscope has a potentiometric output, i.e., dc signal output; however, the signal to noise ratio was too large. Therefore, an amplifier between the gyroscope and telemetry system was built.

4.3 Telemetry System

A Sigma Data Systems telemetry system was used to send the sensor signals to the shore-based computer. The system consists of a transmitter installed on the model, a radio receiver and a reader unit on shore. The time delay from the sensor reading on the model through to the output from the reader was approximately 40ms.

4.4 Data Acquisition

A Strawberry Tree ACJr-12 was used for data acquisition. The card has a maximum of eight channels of which two were used. With two channels used, the card has a sampling rate of 1 kHz at a resolution of 11 bits.

4.5 Computer

A Toshiba T3200 portable computer was used as a host for the data acquisition card and to implement controllers in software. The computer is based on the 16-bit Intel 80286 microprocessor. The operating system used was MS-DOS 4.0. The sampling period used for the controllers was 0.11s. This value, which is constrained by the operating system, when added to the delay time of the telemetry system, results in the closest value to the desired sampling period of 0.13s (Froude scaling of the 0.5s full scale

sampling period).

4.6 Radio Control

The radio control system is based on Futaba R/C components. The
transmitter is a Futaba FP-5FG/K Digital Proportional Radio
Control. It is interfaced with the computer by means of a custom
circuit board between the serial port of the computer and the
trainer port of the R/C transmitter.

The rudder servo on the model has a maximum rudder rate of 91
degrees per second. The constrained rudder rate of 19 degrees
per s (Froude scaling of the 5°/s full scale rudder rate) was
therefore implemented in software.

A diagram of the complete system is provided in Figure 26.
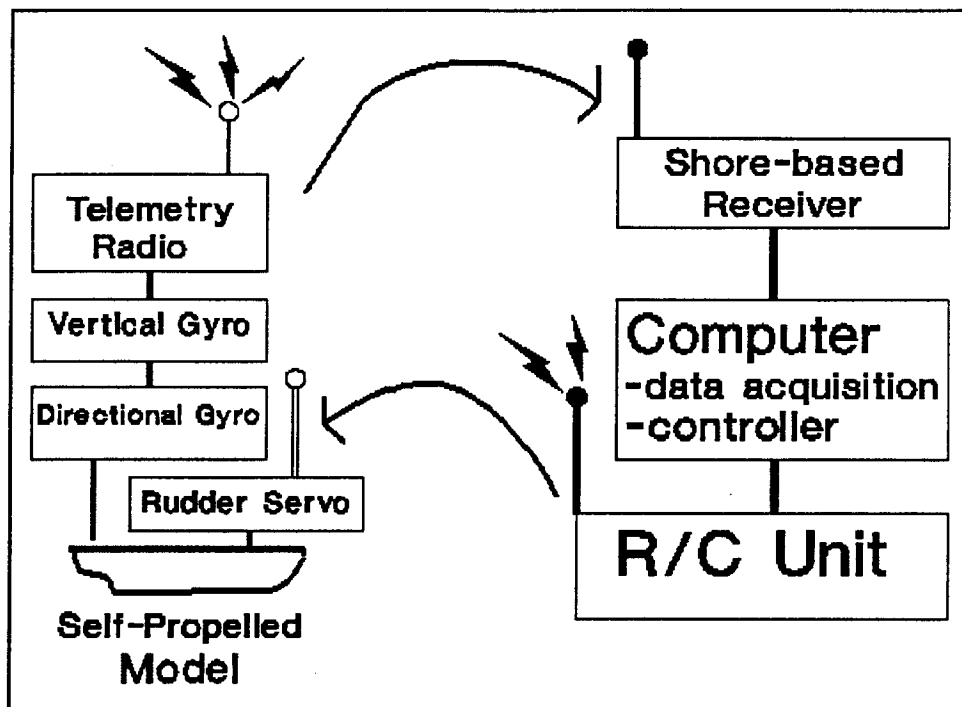
Figure 26. Model Testing Arrangement

4.7 Towing Tank

The location of model testing is the towing tank at the Ocean Engineering Centre at B.C. Research. The tank is 220 feet long, 12 feet wide, and 8 feet deep. Physical model testing was disrupted prior to completion by B.C.Research going into receivership.

4.8 Tests

Only some preliminary tests were completed, due to the loss of the facility. These preliminary tests consisted of nine zig-zag trials, in which only yaw motion was recorded, and one zero-speed roll-decay test.

From the model tests, the yaw rate time constant was found to be around two seconds. The model time constant corresponds to a full scale time constant of around seven seconds. The model tests were made at speeds estimated at three to five knots (full scale). No comparison was made to the numerical model because the numerical model did not produce good responses at these low speeds.

From the roll decay test, the roll natural period was 1.49 seconds and the damping ratio was 0.075. These values were found two ways: first, using logarithmic decrement for the damping ratio and visual measurement of the period, then from regression analysis. The natural period of the model corresponds to a full scale roll period of 5.77 seconds. A comparison to the numerical model roll period was not possible because the GM of the model was not measured. The damping ratio of the physical model is approximately twice that of the numerical model. This discrepancy is most likely due to the bilge keels fitted on the physical model, as it was assumed there were none with the numerical model.

Part 5: Conclusions

1. Based on the results from the numerical simulation, rudder roll reduction does not work well enough for commercial implementation on fishing boats.

2. The yaw motion resulting from the rudder action necessary to reduce roll motion on fishing boats can be too large for rudder roll reduction to be effective.

3. The results from the numerical simulation are suspect because:
   - the results do not indicate better roll response with a faster rudder rate.
   - the results indicate a straighter course gives better roll response.
   - comparison to previous results indicates little difference in the relative capabilities of ships used in these tests and ships used in previous, successful implementations.

4. The VSS, minimum variance, and pole placement controllers had excellent results as autopilots with no roll reduction.

Part 6: Future Work

The research that remains is:

1. Confirm that rudder roll reduction does not work using model tests and the two better rudder roll reduction controllers, i.e., the VSS rudder roll reduction and the pole placement rudder roll reduction controllers.

2. Confirm the autopilot results using model tests.

3. Explore the idea of combining the pole placement and minimum variance controllers into one controller. The resulting controller should have smooth, exact control (like that of the pole placement controller but which the minimum variance tends to lack) without any rudder saturation (which the pole placement has but the minimum variance does not).

Part 6: Bibliography

On Rudder Roll Reduction

1. Roberts, G.N., and S.W. Braham."A Design Study on the Control Of Warship Rolling Motion Using Rudder and Stabilizing Fins." *International Conference on Control* (1991): 838-843.

2. Amerongen, J. van, et al. "Rudder Roll Stabilization for Ships." *Automatica* 26 (1990): 679-690.

3. Amerongen, J. van, et al. "Rudder Roll Stabilization - Controller design and experimental results." *8th Ship Control Systems Symposium Proceedings* 1 (1987): 1.120-1.142.

4. Katebi, M.R., et al. "LQG Autopilot and Rudder Roll Stabilization Control System Design." *8th Ship Control Symposium Proceedings* 3 (1987): 3.69-3.84.

5. Baitis, E., et al. "Rudder Roll Stabilization for Coast Guard Cutters and Frigates." *Naval Engineers Journal* (May 1983): 267-282.

6. Kallstrom, C.G., et al. "Roll Reduction by Rudder Control." *Proceedings 13th STAR Symposium* (1988): 67-76.

7. Kallstrom, C.G. "Control of Yaw and Roll by a Rudder/Fin-Stabilization System." *Proceedings 6th Ship Control Systems Symposium* (1981): F2 3-1-F2 3-23.

On Identification

8. Salgado, M.E., et al. "Modified Least Squares Alogrithm Incorporating Exponential Resetting and Forgetting." *International Journal of Control* 47, No.2 (1988): 477-491.

On Generalized Predictive Control

9. Clarke, D.W., et al. "Generalized Predictive Control - Parts I and II." *Automatica* 23, No.2 (1987): 137-160.

10. Tsang, T.T.C., and D.W. Clarke. "Generalized Predictive Control with Input Constraints." *IEE Proceedings* 135, Pt.D, No. 6 (November 1988): 451-460.

11. Clarke, D.W., and C. Mohtadi. "Properties of Generalized Predictive Control." *IFAC 10th World Congress on Automatic Controls* 10: 63-74.

12. Kinnaert, M. "Adaptive Generalized Predictive Controller for MIMO systems." *International Journal of Control* 50, No.1 (1989): 161-172.

On Sliding Mode Control

13. Müller, P.C. "Stability Analysis of Regular and Sliding Motions of Linear Dynamical Systems with Ideal Relay." *American Control Conference* 3 (1985): 1675-1699.

14. Sarturk, S.Z., et al. "On the Stability of Discrete-Time Sliding Mode Control Systems." *IEEE Transactions on Automatic Control* AC-32, No.10 (October 1987): 930-932.

15. Kotta, U. "Comments on 'On the Stability of Discrete-Time Sliding Mode Control Systems'." *IEEE Transactions on Automatic Control* AC-34, No.9 (September 1989): pp1021-1022.

16. Spurgeon, S.K. "On the Development of Discrete-Time Sliding Mode Control Systems." *International Conference on Control* (1991): 505-510.

17. Spurgeon, S.K. "Hyperplane Design Techniques for Discrete-Time Variable Structure Control Systems." *International Journal of Control* 55, No.2 (1992): 445-456.

On Discrete-Time Control

18. Ogata. K. <u>Discrete-Time Control Systems</u>. Englewood Cliffs: Prentice-Hall Inc., 1987.

19. Isermann, R. <u>Digital Control Systems</u>. Heidelberg: Springer-Verlag, 1981.

For the Numerical Simulation

20. Lewis, E.V. (Editor). <u>Priciples of Naval Architecture Volumes I-III (Second Revision)</u>. Jersey City: The Society of Naval Architects and Marine Engineers., 1988.

21. Bhattacharyya, R. <u>Dynamics of Marine Vehicles</u>. New York: Wiley Interscience, 1978.

22. Inoue, S., et al. "A Practical Calculation Method of Ship Maneuvering Motion." *International Shipbuilding Progress* 28, No.325 (September 1981): 207-222.

23. Inoue, S., et al. "Hydrodynamic Derivatives on Ship Manoeuvring." *International Shipbuilding Progress* 28, No.321 (May 1981): 112-125.

24. Clarke, D., et al. "The Application of Manoeuvring Criteria in Hull Design Using Linear Theory." *Transactions of the Royal Institute of Naval Architects* (1983): 45-68.

25. Bass, D.W., and M.R. Haddara. "Roll and Sway-Roll Damping for Three Small Fishing Vessels." *International Shipbuilding Progress* 38, No.413 (1991): 51-71.

26. Rydill, L.J. "A Linear Theory for the Steered Motion of Ships in Waves." *Transactions of the Royal Institute of Naval Architects* (1959): 81-112.

27. Reid, R.E., et al. "The Use of Wave Filter Design in Kalman Filter State Estimation of the Automatic Steering Problem of a Tanker in a Seaway." *IEEE Transactions on Automatic Control* AC-29, No.7 (July 1984): 577-584.

On PID Autopilots

28. Dickson, Bill, R&D Director, CompuNav Systems. Telephone Conversation with Author, 8 April 1992.

29. Wagner, Paul, Wagner Marine Systems Inc. Telephone Conversation with Author, 8 April 1992.

Appendix I: Approximate Maximum Likelihood Identification

The following is a more detailed description of the identification method used and of the simplification of the identification of the yaw parameters.

Given

$$A(z^{-1}) y = \sum_{i=0}^{j} B_i(z^{-1}) u_i$$

where j is the number of inputs and consider the cross-coupling terms as another form of input.

$$A(z^{-1}) = 1 + a_1 z^{-1} + a_2 z^{-2} + \ldots + a_n z^{-n}$$
$$B(z^{-1}) = b_{0j} + b_{1j} z^{-1} + \ldots + b_{mj} z^{-m}$$

AML identification has the form :

$$P(t+1) = P(t) - \frac{P(t) x_I(t+1) x_I^T(t+1) P(t)}{1 + x_I^T(t+1) P(t) x_I(t+1)}$$

$$K(t+1) = \frac{P(t+1) x_I(t+1)}{1 + x_I^T(t+1) P(t) x_I(t+1)}$$

$$e(t+1) = y(t+1) - x_I^T(t+1) \Theta(t)$$

$$\Theta(t+1) = \Theta(t) + K(t+1) e(t+1)$$

to include the Exponential Forgetting and Resetting algorithm [8] the co-variance and gain equations are modified:

$$P(t+1) = \frac{1}{\lambda} - \frac{\alpha P(t) x_I(t+1) x_I^T(t+1) P(t)}{1 + x_I^T(t+1) P(t) x_I(t+1)} + \beta I - \delta P^2(t)$$

$$K(t+1) = \frac{\alpha P(t+1) x_I(t+1)}{1 + x_I^T(t+1) P x_I(t+1)}$$

x_I is the vector of inputs and outputs.
Θ is the vector of the parameters being estimated.

$$x_I = [-y(k-1), \ldots, -y(k-n), u_1(k-1), \ldots, u_1(k-m_1), \ldots$$
$$, u_2(k-1), \ldots, u_j(K-m_j), \eta(k-1), \ldots, \eta(k-n)]^T$$

$$\Theta = [a_1, a_2, \ldots, a_n, b_{11}, \ldots, b_{1m_1}, b_{12}, \ldots, b_{jm_j}, c_1, \ldots, c_n]^T$$

η are the *a posteriori* errors and

$$\eta(t) = y(t) - \boldsymbol{x}_I^T(t)\boldsymbol{\Theta}(t)$$

For the yaw sub-system, it is assumed n=2, j=2, m_1=1, and m_2=1.

that is

$$(1 + a_1 z^{-1} + a_2 z^{-2})\psi = b_{11} z^{-1} u + b_{12} z^{-1}\phi$$

A simplification for the identification of the yaw subsystem is made by assuming the natural response of yaw is a decay term and an integrator :

$$A(z^{-1}) = (1 - z^{-1})(1 - a_2 z^{-1})$$

$$or \quad a_1 = -(1 + a_2)$$

therefore it is only necessary to identify a_2.

The following changes must be made to x_I and Θ:

$$x_I = [\psi(k-1) - \psi(k-2), u(k-1), \phi(k-1)]^T$$
$$\Theta = [a_2, b_{11}, b_{12}]^T$$
$$e(k) = \psi(k) - \psi(k-1) - x_I^T\Theta$$

Appendix II: Generalized Predictive Control

The following is a more detailed description of the state space generalized predictive controller.

Given a state space system

$$x(k+1) = Ax(k) + Bu(k)$$
$$y(k) = Cx(k)$$

where A is ($n \times n$), B is ($n \times m$), C is ($p \times n$), x is a vector of length n representing the states, u is a vector of length m representing the incremental inputs, and y is a vector of length p representing the outputs.

Assuming a prediction horizon of length N, and a control horizon of length N_u, $N_u \leq N$, the global predictive model is:

$$\Psi = H_{N_u} \tilde{u} + \Psi_0$$

where

$$H_{N_u} = \begin{bmatrix} CB & 0 & \cdots & 0 \\ CAB & CB & \ddots & 0 \\ \vdots & \vdots & \ddots & \vdots \\ \vdots & \vdots & \ddots & CB \\ \vdots & \vdots & \ddots & \vdots \\ CA^{N-1}B & CA^{N-2}B & \cdots & CA^{N-N_u}B \end{bmatrix}$$

$$\Psi_0 = \begin{bmatrix} CA \\ \vdots \\ CA^N \end{bmatrix} x(k)$$

and

$$u_{N_u}(k) = \begin{bmatrix} \Delta u(k) & \Delta u(k+1) & \cdots & \Delta u(k+N_u-1) \end{bmatrix}^T$$

The control law is to choose $\tilde{u}$ which minimizes:

$$J = \Psi^T I_{pN} \Psi + \tilde{u}^T P \tilde{u}$$

where P is a diagonal weighting matrix for the input.

For the case of the rudder with the fixed swing rate, the incremental input has only three possible choices, swing left, swing right, or do not swing. In this case, and assuming a control horizon (N_u) of 1, it is easier to calculate J for each of the three possibilities of input and choose the one which

minimizes J. When the rudder reaches its amplitude constraint, the number of choices decreases to two, decrease the rudder angle or let it remain.

For the case of the rudder with a maximum swing rate, the incremental input which minimizes J is calculated from:

$$\tilde{u} = \left\{ \left[H_{N_U}^T H_{N_U} \right]^{-1} H_{N_U}^T \Psi_0 \right\}$$

The calculated input is then checked against the maximum input and if the calculated value exceeds the maximum, the maximum is implemented. This setting the input to the maximum results from assuming the constrained optimum lies on the boundary of the cost function and the constraint.

Appendix III: Discrete-Time Variable Structure Control

A design equation will be derived for finding the discrete sliding plane co-efficients for a state space system with bounded relay control. The design equation has the form of a matrix Riccati equation.

Given a state space system:

$$\pmb{x}(k+1) = \pmb{A}\pmb{x}(k) + \pmb{B}u(k) \qquad (AIII.1)$$

where **A** is (n×n), **B** is (n×m) and each u_i has the form:

$$u_i(k) = -K_i sign(S_i(k))$$

$$or \; \pmb{u}(k) = -\pmb{K}sign(\pmb{S}(k)) \qquad (AIII.2)$$

$$where \; \pmb{K} = diag(K_i)$$

$$sign(\pmb{S}(k)) = \begin{bmatrix} sign(S_1(k)) \\ \vdots \\ sign(S_m(k)) \end{bmatrix}$$

$$and \; S_i(k) \triangleq G_i x \qquad (AIII.3)$$

where G_i are row vector of size n.

The Ricatti equation will be derived using the second method of Lyaponov.

First, consider the stability of the state trajectories off the sliding subspace using a matrix Lyapanov function :

$$V(x) = x^T(k)Px(k)$$
$$then \quad \Delta V(x) = V(x(k+1)) - V(x(k))$$
$$= x^T(k+1)PX(k+1) - x^T(k)Px(k)$$

using **(AIII.1)**:

$$\Delta V(x) = [Ax(k) + Bu(k)]^T P[Ax(k) + Bu(k)] - x^T(k)Px(k)$$

$$= x^T(k)(A^TPA-P)x(k) + x^T(k)A^TPBu(k)$$
$$+ u^T(k)B^YPAx(k) + u^T(k)B^TPBu(k)$$

using **(AIII.2)**:

$$\Delta V(x) = x^T(k)(A^TPA-P)x(k) - x^T(k)A^TPBKsign(Gx(k))$$
$$- [Ksign(Gx(k))]^TBTPAx(k)$$
$$+ [sign(G(x(k))]^TB^TPB[Ksign(Gx(k))]$$

68

Assume $G = B^T P$:

$$\Delta V(x) = x^T(k)(A^T PA - P)x(k) - x^T(k)A^T PBK sign(B^T Px(k))$$
$$- [Ksign(B^T Px(k))]^T B^T PAx(k)$$
$$+ [Ksign(B^T Px(k))]^T B^T PB[Ksign(B^T Px(k))]$$

Letting $sign(B^T Px(k)) = R^{-1}B^T Px(k)$ where R is an arbitrary weighting matrix of form $diag(r_i)$

$$\Delta V(x) = x^T(k)TPA-P)x(k) - x^T(k)(A^T PBKR^{-1}B^T P)x(k)$$
$$- x^T(k)(PB(R^{-1})^T KB^T PA)x(k)$$
$$+ x^T(k)(PB(R^{-1})^T KB^T PBKR^{-1}B^T P)x(k)$$

Let

$$Q = -[A^T PA - A^T PBKR^{-1}B^T P - PBK(R^{-1})^T B^T PA$$
$$+ PB^T(R^{-1})^T KB^T PBKR^{-1}B^T P]$$

The system is stable if $\Delta V(x)$ is negative definite, $\therefore$ Q must be positive definite. This leads to the following Ricatti equation:

$$P = Q + A^T PA - A^T PBR^{-1}KB^T P - PB(R^{-1})^T KB^T PA \qquad \textbf{(AIII.4)}$$
$$+ PB(R^{-1})^T KB^T PBR^{-1}KB^T P$$

The design procedure is specify a nominal system A,B with control constraints K, and specify the arbitrary weighting matrices Q and R. Then find P from **(AIII.4)**, then $G=B^T P$ and implement $u=-Ksign(Gx(k))$.

69

Appendix IV: Equations of the Transverse Motions

This appendix presents the derivation of the state space equations for the transverse motions of a vessel. The equations will be based on the linear equations of motion. A sample calculation for one speed and loading condition will be performed.

From Inoue et al [22]. (see also v.3, Chapter 9, section 16.7 of [20]) the transverse equations of motion are:

$$Sway \qquad m(\dot{v} + ur) = Y_H + Y_R + Y_W \qquad\qquad (AIV.1)$$

$$Yaw \qquad I_{zz}\dot{r} = N_H + N_R + N_W \qquad\qquad (AIV.2)$$

$$Roll \qquad I_{xx}\ddot{\phi} = K_H + K_R + K_W \qquad\qquad (AIV.3)$$

The force and moments due to wave action ($\cdot_W$) have been added. The free response of the three motions will be developed first, starting with sway (AIV.1) :

$$m(\dot{v}+ur) = -m_y\dot{v} - m_x ur + \frac{1}{2}\rho LdV^2\left[Y_v'\frac{v}{V} + Y_r'\frac{rL}{V}\right] + Y_R + Y_W$$

$$(m+m_y)\dot{v} - \frac{1}{2}\rho LdVY_v'v + (mu + m_x u - \frac{1}{2}\rho L^2 dVY_r')r = Y_R + Y_W$$

Yaw (AIV.2):

$$I_{zz}\dot{r} = -J_{zz}\dot{r} + \frac{1}{2}\rho LdV^2\left[N_v'v' + N_r'r'\right] + \frac{1}{2}\rho L^2 dV^2\left[N_\phi'\phi\right] + N_R + N_W$$

$$(Izz + J_{zz})\dot{r} - \frac{1}{2}\rho LdV\left[LN_v' + Y_v'x_s\right]v - \frac{1}{2}\rho L^2 dV\left[LN_r' + Y_r'x_s\right]r$$

$$- \frac{1}{2}\rho L^2 dV^2 N_\phi'\phi = N_R + N_W$$

Roll (AIV.3):

$$I_{xx}\ddot{\phi} = -J_{xx}\ddot{\phi} - N(\dot{\phi}) - g\Delta GZ(\phi) - Y_H Z_H + K_R + K_W$$

$$(I_{xx} + J_{xx})\ddot{\phi} + N(\dot{\phi}) + g\Delta GZ(\phi) + Y_y Z_H = K_R + K_W$$

Using linear damping and stiffness, as in Bhattacharya [21] :

$$(I_{xx} + J_{xx})\ddot{\phi} + b\dot{\phi} + g\Delta\overline{GM_T}\phi + Y_H Z_H = K_R + K_W$$

Expand Y_H :

$$(I_{xx} + J_{xx})\ddot{\phi} + b\dot{\phi} + g\Delta\overline{GM_T}\phi$$

$$+ \left[-m_y\dot{v} - m_x ur + \frac{1}{2}\rho LdVY_v'v + \frac{1}{2}\rho L^2 dVY_r'r\right]z_H = K_R + K_W$$

$$(I_{xx} + J_{xx})\ddot{\phi} + b\dot{\phi}\ g\Delta\overline{GM_T}\phi - m_y z_H\dot{v} + \frac{1}{2}\rho LdVY_v'z_H v$$

$$+ \left[-m_x u + \frac{1}{2}\rho L^2 dVY_r'\right]z_H r = K_R + K_W$$

Geometries

x_R - The rudder centre of pressure with respect to the ship's centre of gravity. It is measured longitudinally, and is negative aft (see Figure 27).

z_H - Location of the ship's centre of pressure with respect to the ship's centre of gravity. This is the point at which the lateral hydrodynamic forces are assumed to act. Is measured vertically, negative up. For all ships in this study, it was assumed to be on-half the mean draft.

z_R - Location of the rudder's centre of pressure with respect to the ship's centre of gravity. It is measure vertically, and is negative up (see Figure 27).
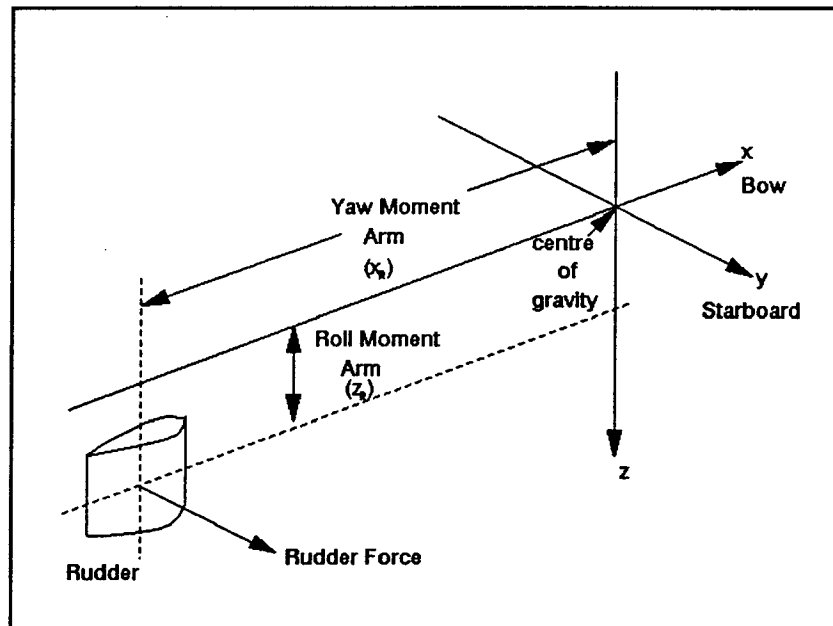
Figure 27. Geomerty of Rudder Moments

Masses and Moments of Inertia

Added mass in the y-direction.
$$m_y = k_2 \, \Delta$$

Added mass in the x-direction
$$m_x = k_1 \, \Delta$$

Added yaw mass moment of inertia
$$J_{zz} = k' I_{zz}$$

The co-efficients, k_1, k_2, and k' are found in Vol.3, Chapter 9, Section 9.4 of [20] . They are based on an ellipsoid of revolution with a major axis of one half the waterline length, and a minor axis of the mean draft.

Yaw mass moment of inertia.

71

The yaw radius of gyration is assumed to be approximately one quarter of the waterline length, i.e.,

$$k_{zz} = 0.25 \ L_{WL}$$

then the yaw mass moment of inertia is

$$I_{zz} = \Delta k_{zz}^2$$

Roll mass moment of inertia.
The roll radius of gyration is assumed to be:

$$k_{xx} = C\sqrt{B^2 + D^2}$$

where C varies between 0.33 and 0.39.

The added roll mass moment of inertia was assumed to be 15% of the mass moment of inertia.

Hydrodynamic Derivatives

The following are the linear hydrodynamic derivatives from Inoue et al. [23]:

$$Y_v' = -\left(\frac{1}{2}\pi k + 1.4 C_B \frac{B}{L}\right)\left(1.0 + \frac{2\tau}{3T}\right)$$

$$Y_r' = \frac{1}{4}\pi k\left[1 + 0.8\frac{\tau}{T}\right]$$

$$N_v' = -k\left[1 - \frac{0.27\tau}{l_\beta T}\right]$$

$$N_r' = -[0.54k - k^2]\left[1.0 + 0.3\frac{\tau}{T}\right]$$

$$where \quad k = \frac{2T}{L_{PP}}$$

$$l_\beta = \frac{k}{\left[\frac{1}{2}\pi k + 1.4 C_B \frac{B}{L}\right]}$$

$$\tau = T_{AFT} - T_{FWD}$$

The roll damping coefficient depended on the hull form. For hard chine hulls a damping ratio of 0.09 [25] was used. For round bilge

hulls the following formulae, from [20] were used:

$$\zeta_0 = \frac{0.55\left(.0024\,LBd^{\frac{1}{2}}\right)d^{\frac{5}{2}}\phi^{\frac{1}{2}}}{\Delta B^2}$$

$$\zeta_f = 0.00085\left(\frac{L}{B}\right)\left(\frac{L}{GM}\right)^{\frac{1}{2}}\left(\frac{Fn}{C_B}\right)\left[1 + \frac{Fn}{C_B} + 2\left(\frac{Fn}{C_B}\right)^2\right]$$

$$\zeta = \zeta_0 + \zeta_f$$

where

ζ_0 – *zero speed damping ratio*

ζ_f – *forward speed correction*

Fn – *Froude Number* $= \dfrac{V}{\sqrt{gL}}$

d – *distance the intersection of the waterline and centreline to the turn of the bilge*

The critical roll damping was found from:

$$b_c = 2\sqrt{g\Delta\overline{GM_T}(I_{xx} + J_{xx})}$$

Rudder Forces

The rudder forces and moments are :

$$Y_R = -(1 + a_H)F_N\cos\delta$$
$$N_R = -(1 + a_H)x_R F_N\cos\delta$$
$$K_R = (1 + a_H)z_R F_N\cos\delta$$

where

$$F_N = \frac{1}{2}\rho\,\frac{6.13\lambda}{\lambda+2.25}A_R V_R^2\sin\alpha_R$$
$$a_H = 0.627\,C_B - 0.153$$

The method for finding V_R in Inoue et al. is quite complicated, so

73

instead equation (169) from Vol.3, Chapter 9 of [20] was used :

$$V_R = k(1 + Sa)V$$

where $0.8 < k < 1.0$ *depending how much of the rudder is in the propeller slipstream.*

$$Sa = \frac{Pn - V}{Pn}$$

where   *P - propeller pitch*
n - rev / unittime
V - Ship velocity

For α_R, assume $\alpha_R \approx \delta$.   Also, it was assumed $\cos(\delta) \approx 1$.

Sample Calculations

The following are the necessary parameters needed to calculated the transverse motion co-efficients.

Vessel name & Condition: *Eastward Ho* Full load 13kts

Ship Data

Lwl	30.7848	Cb	0.513686
Bwl	8.738616	L/B	3.522846
Depth	4.2672	B/T	2.163774
Taft	4.54025	B/D	2.047857
Tfwd	3.4671		
Tmean	4.0386		
tau	1.07315		
Displ (Vol.)	558.094		
Displ (Mass)	572.0463		

Engine		Propeller	
Type		Dia.	2.1336
Bhp	850	Pitch	1.524
RPM	1225	k	0.99
Gear Red	4	RPM	300

	knots	m/s
Speed	13	6.68772
Fn	0.384836	

Stability		x - positive fwd;	
		z - positive down	
LCG	-1.8928	VCG	3.377184
GM	1.267968	zh	1.357884 below c.g.

Round bilge or Hard Chine (b or c)   b
distance from C.L. @ W.L. to turn of bilge 4.60

```
Rudder
height        2.286        xr       -12.509
Span          2.286        zr       2.36584
Chord         1.2192
Area          2.787091
Aspect Ratio       1.875
```

The added masses, mass moments of inertia and hydrodynamic derivatives were calculated using the above formulae:

```
Added Mass x-direction      45.04215

Added Mass y-direction      494.4331

Yaw Radius of Gyration       7.6962

Yaw Mass Moment of Inertia 33883.16

Added yaw m.m. of i.        19587.96

Roll Radius of Gyration      3.50094

Roll Mass Moment of Inertia7011.333

Added Roll M.M. of I.       1402.267

Zero Speed Roll Damping
Coefficient                 0.011913
Roll Damping                675.5547

k                           0.262376
L-beta                      0.425741

Yv prime                    -0.72545

Yr prime                    0.249876

Nv prime                    -0.21816

Nr prime                    -0.07865

Nphi prime                   -0.0076
For the rudder forces:
  Sa                        0.122346
  Rudder Velocity           7.430879
  Rudder Normal Force       219.7674
  ah                        0.169081
```

The co-efficients for the equations of motion are then found to be:

```
Sway Equation
  Sway acceleration         1066.479
  Sway Velocity              309.136
  Yaw rate                  848.9842
```

Yaw Equation
    Yaw Acceleration   53471.11
    Yaw Rate   25557.17
    Sway Velocity   3447.02
    Roll Angle   666.7563

Roll Equation
    Roll Acceleration   8413.6
    Roll Velocity   675.5547
    Roll Angle   7115.55
    Sway Acceleration   -671.383
    Sway Velocity   -419.771
    Yaw Rate   4042.015

Rudder forces
    Sway   -256.926
    Yaw   3213.883
    Roll   607.8455

The co-efficents are then arranged into proper matrices A and B:
where the state vector is:

Ac
        0   1   0   0   0
        0 -0.47796 -0.06447 -0.01247   0
        0 -0.79606 -0.28987   0   0
        0   0   0   0   1
        0 -0.54394 0.026761 -0.84572 -0.08029

Bc
        0
0.060105
-0.24091
        0
0.053022

Kc
        0   0   0
        1   0   0
        0   1   0
        0   0   0
        0 0.197267   1

These matrices are discretized using a zero order hold to obtain
the discrete time matrices:

A
1 0.445675 -0.00711 -0.00142   0
0 0.792773 -0.02667 -0.00535   -0.0014
0 -0.32935 0.870468 0.001073   0
0 -0.06138 0.003745 0.897635 0.473025
0 -0.23094   0.01553 -0.39928 0.859656

B
0.007248
0.028484
-0.11763
0.005723
0.020789

K
0.11573 -0.00122   0
0.445675 -0.00713   0
-0.08775 0.466396   0
-0.01052 0.010064 0.121193
-0.06138 0.040641 0.473025

A comparison between the continuous time model (using a Runge-Kutta differential equation solver) and the discrete time model is given in the following figures. As can be seen in the figures, not only do both models seem to be reasonable representations of the transverse motions, for the purposes of this study the difference between them is unmeasureable.
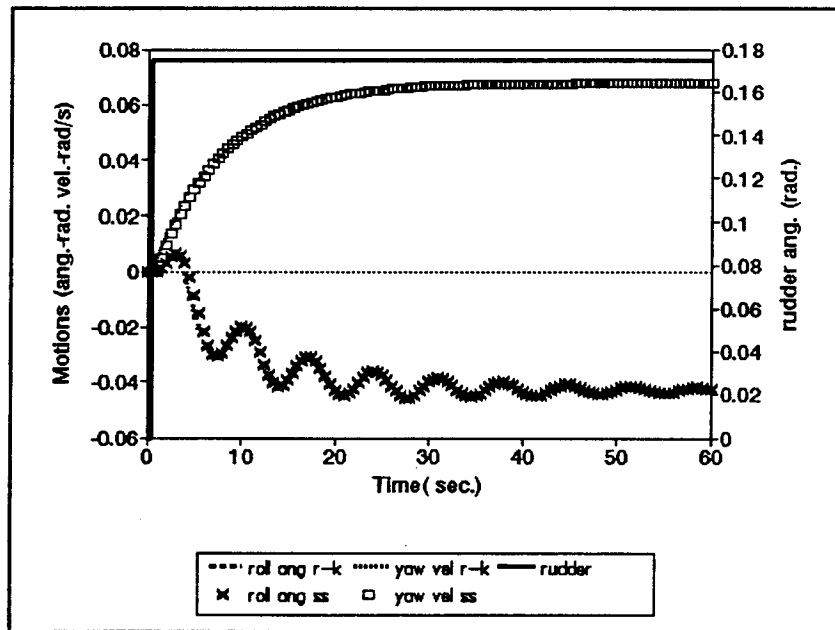
Figure 28. 10° Rudder Step Response.
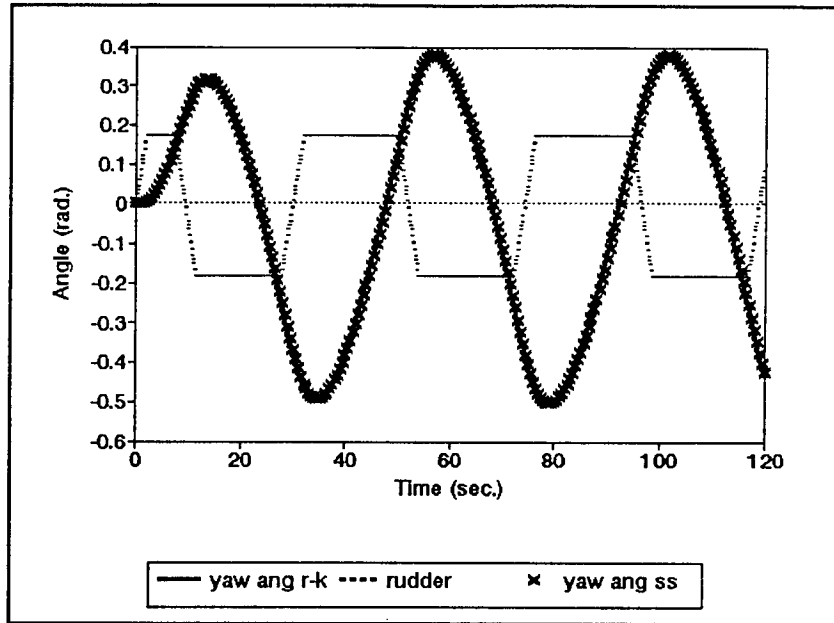
Figure 29. 10°/10° Zig-zag, rudder and yaw.
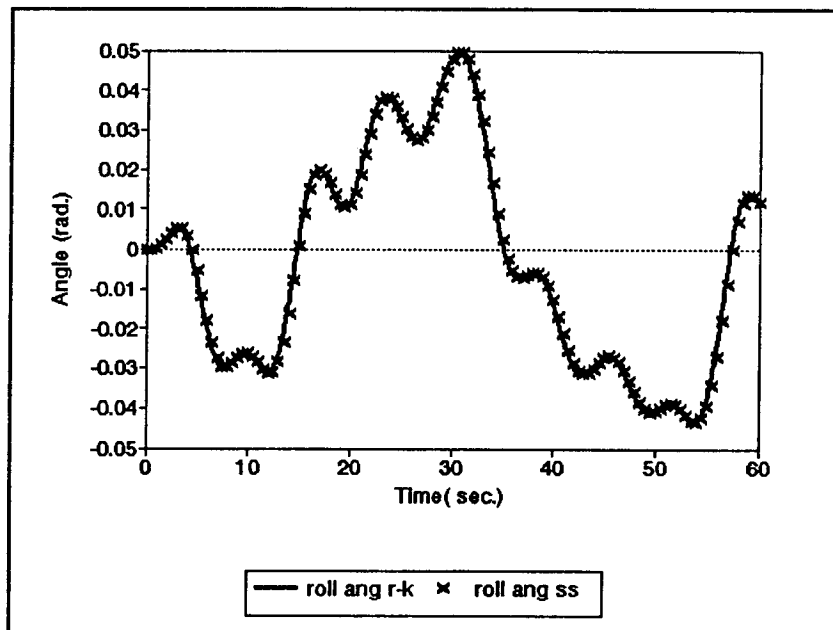
Figure 30. 10°/10° Zig-zag, roll.

78

Appendix V: Wave Excitation

The wave action on a ship is highly non-linear, and is not easily simplified. This appendix describes the steps used to obtain a numerical model of wave excitation for implementation in a discrete simulation. The excitation is usually represented as a force or moment equation that is dependent on frequency. From these equations, digital filters must be obtained that have as their inputs white noise.

From ref. 26, the sway excitation force is :

$$Y_w = \rho g e^{-kz} \sin\chi \int_L A_x \cos(k'x)\, dx \; \xi_m \sin(\omega_e t)$$

and the yaw excitation moment is:

$$N_w = -\rho g e^{-kz} \sin\chi \int_L A_x x \sin(k'x)\, dx \; \xi_m \cos(\omega_e t)$$

where

Z = *distance of the $\overline{CB}$ below the waterline*
k' = $k\cos\chi$
k = *the wave number*
χ = *the wave encounter angle ($0°$ following seas, $180°$ head seas)*
ω_e = *wave encounter frequency*

$$A_x = \frac{1}{2}\pi\left(T^2 - \frac{4\pi x^2}{L^2} \right)$$

In this simulation, the cross-sectional area A_x is that of an ellipsoid of revolution, with the minor axis equal to the draught and the major axis equal to one half the length.

From [21] , the roll excitation moment is:

$$K_w = g\Delta\overline{GM_T}\sin\chi \; \xi\sin(\omega_e t)$$

The wave slope spectrum used in this simulation is based on the Bretschneider Spectrum (wave height):

$$S(\omega) = \frac{A}{\omega^5} e^{-\frac{B}{\omega^4}}$$

where A and B depend on the modal frequency and variance. For wave slope spectrum, the Bretscneider Spectrum is modified:

$$S_\xi(\omega) = \frac{\omega^4}{g^2} S(\omega) = \frac{A}{\omega g^2} e^{-\frac{B}{\omega^4}}$$

The spectrum must be further modified so it is based on the frequency of encounter ω_e:

$$S_\xi(\omega_e) = \frac{S_\xi(\omega)}{\left|1 - \dfrac{2\omega U}{g}\cos\chi\right|}$$

where:

$$\omega_e = \left|\omega - \frac{\omega^2 U}{g}\cos\chi\right|$$

All of the forces and moments are an amplitude multiplied by the wave slope $\xi\sin(\omega_e t + \epsilon)$; however, both the sway and yaw amplitudes are functions of the wave number and hence the wave frequency. Therefore the spectra of these amplitudes must be found. They have the form:

$$S_e(\omega_e) = \left|M_e(\omega_e)\right|^2 S_\xi(\omega_e)$$

This complicates the calculation of the spectrum. Because each ω_e has three corresponding values of ω, the amplitudes and wave slopes must be calculated for each of the three frequencies, multiplied, then summed (see ref).

These spectra were then approximated by continuous time transfer functions whose power spectra were matched for shape visually and area under their curves quantitatively.

The transfer functions were discretized using the bi-linear transform with the appropriate sampling period.

For beam seas (χ=90), the excitation was further simplified. The sway excitation force used in this case was:

$$Y_w = \frac{mg}{m + m_y}\xi\sin(\omega_e t)$$

The yaw excitation was taken to be zero because the hull shape approximation of an ellipsoid of revolution means the hull has fore-aft symmetry resulting in zero net excitation.

The roll excitation remained the same.

The only necessary spectrum calculation was then for wave slope, and in beam seas there is no complication with different wave frequencies for encounter frequency, i.e. $\omega=\omega_e$.

Appendix VI: Numerical Simulation Results

Kynoc 15° Offset

Controller	Final yaw angle	Maximum yaw angles		Settling time (s)	Rise Time (s)
PID	8.50e-08	-2e-06	9e-06	45	5.5
MV	0.125072	-5e-05	5e-05	20.5	20.5
MV RRS	-0.38812	-2e-04	2e-04	27.5	11.5
BB GPC	-0.90094	-2e-04	2e-04	22	6
BB GPC RRS	-0.38774	-5e-05	4e-05	42.5	7.5
VSS	0.638019	-3e-05	3e-05	20.5	18.5
VSS RRS	0.125071	-5e-05	5e-05	33.5	7
Pole Plc	-4.0e-09	-2e-06	2e-06	16	13.5
Pole RRS	0	0	0	23.5	12
SS GPC	1.00e-09	-2e-06	2e-06	21	7
SS GPC RRS	-2.4e-07	-3e-04	3e-04	43.5	7.5

Kynoc 5.7°/s Impulse

Controller	Final yaw angle	Maximum Yaw angles		Settling time (s)	Rise Time (s)
PID	2.10e-08	-2e-06	5e-06	44	5.5
MV	-0.08354	-5e-06	4e-06	27.5	13.5
MV RRS	0.429435	-6e-05	4e-05	39	7
BB GPC	0.942373	-6e-05	5e-05	30	4
BB GPC RRS	-0.08349	-4e-05	4e-05	27	5
VSS	0.429384	-5e-06	3e-06	27.5	18.5
VSS RRS	-0.0836	-4e-05	5e-05	47.5	10.5
Pole Plc	-1.2e-08	-6e-06	4e-06	27	7
Pole RRS	0	0	0	33.5	6.5
SS GPC	-9.0e-09	-3e-06	2e-06	25	5
SS GPC RRS	0	0	0	23	5

81

Kynoc Change in Speed

Controller	Final yaw angle	Maximum yaw angles		Settling time (s)	Rise Time (s)
PID	0.000968	−0.025	0.06	112.5	118
MV	0.137847	−3e-05	3e-05	18.5	8.5
MV RRS	−0.09171	−8e-05	9e-05	41.5	11.5
BB GPC	−0.01489	−0.393	0.389	599	6.5
BB GPC RRS	−0.09163	−2e-05	2e-05	32	8.5
VSS	−0.55074	−1e-04	1e-04	22.5	13.5
VSS RRS	−0.09163	−2e-05	2e-05	20	18.5
Pole Plc	−3.0e-09	−2e-06	2e-06	19	8.5
Pole RRS	0	0	0	31	10
SS GPC	−6.0e-09	−3e-06	2e-06	30	7.5
SS GPC RRS	−2.6e-08	−1e-05	8e-06	33	8.5

Kynoc Change in Displacement

Controller	final yaw angle	Maximum Yaw Angles		Settling time (s)	Rise Time (s)
PID	−8.2e-08	−2e-05	3e-05	49	5.5
MV	−0.3404	−4e-05	7e-05	35.5	13.5
MV RRS	0.199443	−5e-05	9e-05	44	10
BB GPC	−0.88027	−1e-04	2e-04	48	4.5
BB GPC RRS	0.199578	−6e-05	5e-05	38	4.5
VSS	0.199515	−2e-05	3e-05	35.5	22
VSS RRS	0.199452	−3e-04	6e-04	78	12
Pole Plc	7.80e-08	−3e-05	4e-05	35.5	6.5
Pole RRS	0	0	0	31.5	6.5
SS GPC	2.50e-08	−1e-05	2e-05	33	5
SS GPC RRS	−1.0e-09	−1e-06	1e-09	34.5	4.5

Kynoc Change in Speed and Displacemnt

Controller	Final yaw angle	Maximum Yaw angles		Settling time (s)	Rise Time (s)
PID	0.000507	-0.048	0.108	118	9
MV	-0.72037	-3e-05	3e-05	22.5	8
MV RRS	-0.20882	-3e-05	8e-05	45.5	11.5
BB GPC	-0.28261	-10.03	11.2	186	7
BB GPC RRS	0.047001	-6e-05	3e-05	55.5	8.5
VSS	1.069895	-1e-04	1e-04	22	16.5
VSS RRS	-0.20894	-1e-04	1e-04	31.5	14.5
Pole Plc	-9.0e-09	-1e-05	1e-05	24.5	7.5
Pole RRS	0	0	0	36	8
SS GPC	-2.9e-08	-2e-05	2e-05	37.5	7.5
SS GPC RRS	3.05e-07	-0.002	0.002	53	8

Kynoc Rudder Servo Slows

Controller	Final yaw angle	Maximum Yaw Angles		Settling time (s)	Rise Time (s)
PID	2.30e-08	-2e-06	5e-06	44.5	599.5
MV	-0.18619	-5e-05	5e-05	27.5	13.5
MV RRS	-0.18596	-1e-04	1e-04	28.5	7.5
BB GPC	-1.00688	-5e-05	5e-05	21	4.5
BB GPC RRS	-0.18634	-2e-04	2e-04	27	5.5
VSS	0.634489	-5e-05	5e-05	27.5	15
VSS RRS	-0.18619	-5e-05	5e-05	35.5	11.5
Pole Plc	-1.0e-08	-5e-06	4e-06	27	11.5
Pole RRS	0	0	0	31.5	6.5
SS GPC	-9.0e-09	-3e-06	2e-06	23	5.5
SS GPC RRS	0	0	0	24.5	5.5

Kynoc Constant Yaw Moment

Controller	Final yaw angle	Maximum Yaw Angle		Settling time (s)	Rise Time (s)
PID	-1.9e-06	-1e-06	3e-06	40.5	94
MV	3.042305	-3.162	10.99	595.5	5.5
MV RRS	148.3223	-126.2	179	520	76.5
BB GPC	0.760904	-3.342	3.932	530.5	5.5
BB GPC RRS	25.81668	-162.8	180.3	593	7
VSS	-0.1463	-0.132	0.129	597.5	16
VSS RRS	-3.4502	-0.143	0.133	599.5	6.5
Pole Plc	0.613604	-1.095	1.169	583.5	32
Pole RRS	0.824794	-11.78	5.514	584	10.5
SS GPC	0.562783	-0.326	0.331	599	35
SS GPC RRS	14.26879	-118.4	135.1	599.5	7.5

The column %PID, in the tables of the irregular sea test results, is the amount of roll reduction using a controller as compared to using the PID controller.

Kynoc 90° Seas

Controller	RMS rudder angle	RMS yaw angle	Maximum yaw angles		RMS roll angle	Maximum roll angle		%PID
PID	1.68	1.53	-5.61	3.39	2.78	-8.28	8.45	0.0%
MV	6.42	1.56	-5.12	5.71	3.37	-9.49	10.4	-21.3%
MV RRS	5.68	1.64	-4.67	6.28	3.45	-9.07	9.27	-24.0%
BB GPC	7.44	2.41	-9.08	10.9	3.3	-10.5	8.97	-18.7%
BB GPC RRS	7.32	3.35	-13.4	11.9	2.82	-8.08	10.5	-1.3%
VSS	4.98	1.07	-3.58	4.94	3.23	-9.74	8.51	-16.1%
VSS RRS	4.68	1.72	-5.22	6.15	1.76	-5.27	5.11	36.8%
Pole Plc	4.5	1.14	-5.54	4.37	3.28	-9.53	10.4	-17.9%
Pole RRS	5.52	3.14	-10.3	12.6	3.03	-9.93	11.1	-8.9%
SS GPC	2.47	1.17	-3.46	3.86	2.82	-7.86	8.37	-1.5%
SS GPC RRS	5.09	1.91	-6.68	4.88	2.22	-5.74	8.05	20.1%

Kynoc 45° Seas

Controller	RMS rudder angle	RMS yaw angle	Maximum yaw angle		RMS roll angle	Maximum roll angle		%PID
PID	2.36	2.19	-5.71	5.36	2.59	-6.84	6.99	0.0%
MV	2.08	0.27	-0.87	0.91	1.34	-3.57	3.95	48.3%
MV RRS	2.3	1.37	-5.22	4.45	2.43	-7.11	8.05	6.2%
BB GPC	2.19	0.42	-1.36	1.75	1.57	-3.48	4.48	39.3%
BB GPC RRS	3.35	2.73	-9.85	8.93	2.37	-7.31	8.35	8.5%
VSS	1.93	0.27	-0.85	0.67	1.3	-3.52	4.5	49.9%
VSS RRS	5.27	5.91	-16.3	15.9	3.46	-10.5	9.84	-33.6
Pole Plc	1.87	0.48	-2.11	2.08	1.61	-4.4	5.25	37.9%
Pole RRS	2.42	1.13	-4.14	4.37	2.09	-9.85	8.48	19.3%
SS GPC	2.41	0.88	-3.57	3.34	2.1	-7.65	7.38	18.9%
SS GPC RRS	3.13	1.24	-3.47	7.35	3.12	-10.4	9.68	-20.6

Kynoc 60° Seas

Controller	RMS rudder angle	RMS yaw angle	Maximum yaw angle		RMS roll angle	Maximum roll angle		%PID
PID	2.17	1.94	-6.67	5.43	2.56	-8.98	8.81	0.0%
MV	2.78	0.4	-1.43	1.91	2.03	-6.53	6.46	20.5%
MV RRS	3.15	1.46	-6.21	4.75	3.03	-9.02	8.66	-18.4
BB GPC	2.64	0.51	-1.92	1.8	2.54	-8.33	7.8	0.6%
BB GPC RRS	3.64	2	-9.41	7.12	3.14	-9.4	9.91	-22.9
VSS	2.78	0.59	-2.27	1.91	2.29	-6.89	8.33	10.6%
VSS RRS	5.18	5.64	-12.7	19.4	3.03	-8.4	8.38	-18.3
Pole Plc	2.18	0.61	-3.06	1.5	2.16	-6.92	6.05	15.6%
Pole RRS	2.46	1.09	-2.87	3.21	2.09	-6.99	6.28	18.2%
SS GPC	2.34	0.85	-2.87	2.43	2.37	-6.43	7.18	7.2%
SS GPC RRS	4.08	1.42	-4.15	8.5	4.24	-14.4	11	-65.9

85

Kynoc 30° Seas

Controller	RMS rudder angle	RMS yaw angle	Maximum yaw angle		RMS roll angle	Maximum roll angle		%PID
PID	1.63	1.44	-4.98	4.66	1.34	-3.9	4.81	0.0%
MV	5.71	1.03	-5.08	4.37	1.9	-5.57	5.2	-41.6%
MV RRS	4.81	0.85	-2.67	3.35	1.85	-5.89	4.88	-38.2%
BB GPC	6.89	1.85	-6.01	9.23	1.85	-4.9	6	-38.0%
BB GPC RRS	4.37	1.72	-5.23	6.74	1.45	-4.58	4.61	-7.8%
VSS	4.55	0.53	-2.68	2.41	1.65	-4.46	4.1	-22.8%
VSS RRS	3.43	1.84	-5.06	4.7	1.21	-2.95	3.51	9.8%
Pole Plc	3.78	1.02	-8.71	3.72	1.61	-4.07	6.23	-19.7%
Pole RRS	3.01	0.86	-3.42	2.53	1.35	-3.95	5.33	-0.6%
SS GPC	2.1	0.92	-2.59	3.43	1.38	-4.23	3.93	-3.1%
SS GPC RRS	3.93	1.05	-3.27	3.26	1.5	-4.62	4.6	-11.7%

Eastward Ho 15° Offset

Controller	Final yaw angle	Maximum yaw angles		Settling time (s)	Rise Time (s)
PID	-7e-06	-0.0006	0.0002	61.5	9.5
MV	-0.5592	-5e-05	0.0002	57.5	29.5
MV RRS	-0.7745	-141.09	142.86	599.5	9.5
BB GPC	-0.0004	-0.7497	0.7434	599.5	7
BB GPC RRS	0.00436	-4.1305	3.1941	173	7.5
VSS	-0.5593	-0.0002	0.0005	45	20.5
VSS RRS	-0.0035	-7e-05	5e-05	54.5	10
Pole Plc	-0.0006	-0.0283	0.0088	112.5	13
Pole RRS	3.0e-06	-1e-05	0.0001	61	18
SS GPC	1.6e-07	-0.0001	0.0002	46.5	7.5
SS GPC RRS	-7e-05	-0.3572	0.3867	125	7.5

Eastward Ho 5.7°/s Impulse

Controller	Final yaw angle	Maximum yaw angles		Settling time (s)	Rise Time (s)
PID	−6e−06	−0.0007	0.0002	53	11.5
MV	−0.6879	−0.0003	0.0004	52.5	26.5
MV RRS	−3.5587	−141.76	150.63	588.5	23
BB GPC	0.7869	−62.223	61.5	599.5	13
BB GPC RRS	−0.176	−5.9902	4.4323	215.5	20
VSS	−0.1325	−0.0003	0.0007	37.5	27.5
VSS RRS	−0.1321	−0.0002	0.0066	86.5	13.5
Pole Plc	0.00013	−0.0162	0.0488	105.5	19
Pole RRS	8.5e−06	−4e−05	0.0005	64.5	27
SS GPC	−0.4564	−53.359	56.018	599.5	13
SS GPC RRS	−0.0215	−1.4335	1.4286	188	18

Eastward Ho Change in Speed

Controller	Final yaw angle	Maximum yaw angles		Settling time (s)	Rise Time (s)
PID	0.00002	−0.0072	0.0213	82	18.5
MV	0.02614	−0.0002	0.0019	59.5	94
MV RRS	0.39059	−61.347	62.129	588.5	31
BB GPC	−0.0496	−41.354	37.701	599	17.5
BB GPC RRS	0.15408	−23.311	24.146	410.5	25
VSS	0.32531	−0.0008	0.0003	42	11
VSS RRS	0.02617	−9e−05	0.0028	70.5	20
Pole Plc	0.00237	−0.0476	0.1434	113	21.5
Pole RRS	0.0001	−0.0005	0.0043	71	29.5
SS GPC	−0.1898	−35.549	34.262	599.5	17.5
SS GPC RRS	0.30052	−25.041	25.199	599.5	25

Eastward Ho Change in Displacement

Controller	Final yaw angle	Maximum yaw angles		Settling time (s)	Rise Time (s)
PID	-7e-06	-0.001	0.0005	63.5	12
MV	-0.7322	-0.0005	0.0012	56	34.5
MV RRS	-0.1813	-16.977	14.463	599.5	25
BB GPC	0.63329	-52.121	53.6	593.5	13.5
BB GPC RRS	0.19987	-21.275	10.783	398	22
VSS	0.23758	-0.0002	0.0005	40	14
VSS RRS	0.23783	-0.0004	5e-05	64.5	12.5
Pole Plc	0.00021	-0.0146	0.048	105.5	19.5
Pole RRS	0.00001	-0.0001	0.0013	64.5	26.5
SS GPC	0.61526	-52.615	52.128	599.5	13.5
SS GPC RRS	-0.4353	-43.571	42.295	595	19

Eastward Ho Change in Speed and Displacement

Controller	Final yaw angle	Maximum yaw angles		Settling time (s)	Rise Time (s)
PID	0.00075	-0.0133	0.0498	89	20.5
MV	0.89277	-0.001	0.0008	45	24.5
MV RRS	0.35148	-7.8573	11.842	567.5	31.5
BB GPC	0.5361	-37.423	37.03	588.5	19
BB GPC RRS	0.02525	-21.816	21.485	597	26.5
VSS	0.43468	-20.182	19.51	599.5	12
VSS RRS	0.09858	-0.0057	0.0002	75.5	22.5
Pole Plc	-0.0015	-0.1442	0.2244	121.5	19.5
Pole RRS	0.00051	-0.005	0.0293	85.5	29.5
SS GPC	-0.3188	-34.427	35.615	591	19
SS GPC RRS	0.41512	-31.58	29.617	593.5	27

Eastward Ho Rudder Servo Slows

Controller	Final yaw angle	Maximum yaw angles		Settling time (s)	Rise Time (s)
PID	-6e-06	-0.0007	0.0002	53	11.5
MV	-0.3545	-0.0002	0.0004	58.5	34.5
MV RRS	3.77801	-172.25	165.01	599.5	24.5
BB GPC	-2.0863	-92.61	93.464	599.5	12
BB GPC RRS	0.06609	-2.5976	2.3221	325.5	22
VSS	-0.3546	-0.0001	0.0004	38.5	21
VSS RRS	0.09006	-0.0006	3e-05	69	13.5
Pole Plc	0.00013	-0.0162	0.0488	105.5	19
Pole RRS	0.00001	-8e-05	0.001	65.5	26.5
SS GPC	0.50356	-81.621	82.572	594.5	12
SS GPC RRS	-3.0707	-60.934	62.794	599.5	19

Eastward Ho Constant Yaw Moment

Controller	Final yaw angle	Maximum yaw angles		Settling time (s)	Rise Time (s)
PID	2.30345	-7e-05	8e-05	56.5	2
MV	-1.2041	-1.5041	.1.3088	599.5	24.5
MV RRS	125.524	-113.83	161.42	599.5	351.5
BB GPC	0.19339	-0.1952	0.2128	599.5	6
BB GPC RRS	-2.005	-8.6811	11.364	577	5
VSS	0.07789	-0.1144	0.0831	596.5	11.5
VSS RRS	-0.5758	-0.115	0.1003	596.5	13
Pole Plc	0.54117	-0.458	0.6232	599.5	147
Pole RRS	0.62503	-6.2533	6.4285	599.5	12
SS GPC	0.11393	-0.1941	0.2111	475	7.5
SS GPC RRS	-7.709	-5.606	8.5922	599.5	56.5

Eastward Ho 90° Seas

Controller	RMS rudder angle	RMS yaw angle	Maximum yaw angles		RMS roll angle	Maximum roll angles		%PID
PID	0.79	0.741	-1.71	2.34	4.264	-12.5	10.6	0.0%
MV	4.42	0.564	-1.69	1.81	3.649	-12.3	12.6	14.4%
MV RRS	23	40.66	-105	84.2	4.013	-12.6	12.4	5.9%
BB GPC	22.8	19.32	-42.2	39.9	4.632	-13.1	12.7	-8.6%
BB GPC RRS	26.8	23.7	-42.9	44.4	5.749	-16.1	18.7	-34.8%
VSS	6.73	0.831	-4.09	2.96	3.873	-10.6	11.1	9.2%
VSS RRS	5.33	2.043	-6.67	6.42	4.112	-12.1	12.1	3.6%
Pole Plc	0.39	0.83	-1.81	2.9	3.748	-9.93	9.94	12.1%
Pole RRS	12.8	20.51	-66.6	45.8	4.509	-11.9	11.9	-5.7%
SS GPC	20.3	16.29	-37.4	38.3	4.557	-13.1	13.2	-6.9%
SS GPC RRS	25.4	20.46	-39.4	37.1	4.272	-13	11	-0.2%

Eastward Ho 45° Seas

Controller	RMS rudder angle	RMS yaw angle	Maximum yaw angles		RMS roll angle	Maximum roll angle		%PID
PID	1.68	1.639	-3.91	3.88	0.929	-2.66	3.14	0.0%
MV	2.17	0.464	-1.26	1.45	0.97	-2.56	3.36	-4.5%
MV RRS	2.63	2.821	-9.94	7.5	1.024	-3.37	3.2	-10.2%
BB GPC	2.76	0.318	-1.52	0.81	1.177	-2.85	3.78	-26.7%
BB GPC RRS	7.43	3.68	-18.6	15.5	2.375	-6.25	5.89	-156%
VSS	2.21	0.105	-0.37	0.25	0.859	-2.59	2.69	7.5%
VSS RRS	3.12	2.847	-6.39	7.61	0.828	-2.02	2.03	10.9%
Pole Plc	2.16	2.341	-6.55	6.08	0.913	-3.46	2.96	1.7%
Pole RRS	2.32	1.091	-3.46	3.79	0.923	-2.89	4.93	0.6%
SS GPC	2.7	0.395	-1.49	1.4	1.06	-3.47	2.96	-14.1%
SS GPC RRS	4.16	0.863	-3.61	3.33	1.812	-5.71	5.65	-95.1%

90

Eastward Ho 60° Seas

Controller	RMS rudder angle	RMS yaw angle	Maximum yaw angles		RMS roll angle	Maximum roll angles		%PID
PID	1.78	1.72	−4.96	4.53	1.959	−4.71	6.34	0.0%
MV	2.75	0.487	−1.26	1.35	1.955	−6.03	7.03	0.2%
MV RRS	2.47	2.394	−9.44	7.29	1.64	−4.25	4.74	16.3%
BB GPC	3.14	0.38	−1.84	1.19	1.91	−6.32	7.02	2.5%
BB GPC RRS	5.99	2.367	−8.47	8.27	2.855	−7.8	7.27	−45.8%
VSS	2.71	0.118	−0.39	0.32	1.629	−5.05	5.03	16.8%
VSS RRS	4.15	3.62	−9.16	9.29	1.267	−4.17	3.7	35.3%
Pole Plc	2.15	2.726	−6.34	8.06	1.639	−4.55	5.27	16.3%
Pole RRS	4.24	2.633	−8.05	7.95	1.634	−6.94	6.14	16.6%
SS GPC	2.9	0.457	−2.06	1.92	1.663	−4.41	4.4	15.1%
SS GPC RRS	4.82	1.177	−5.9	5.29	2.537	−6.66	7.68	−29.5%

Eastward Ho 30° Seas

Controller	RMS rudder angle	RMS yaw angle	Maximum yaw angles		RMS roll angle	Maximum roll angles		%PID
PID	0.84	0.809	−2.08	1.68	1.004	−2.95	4.02	0.0%
MV	3.03	1.393	−2.61	5.26	1.159	−3.48	3.13	−15.4%
MV RRS	2.08	0.737	−2	2.81	1.004	−3.47	3.19	0.0%
BB GPC	24.2	21.6	−42.1	40.5	2.474	−5.69	5.22	−146%
BB GPC RRS	7.53	1.998	−6.61	6.04	1.968	−5.34	4.88	−96%
VSS	4.66	0.212	−0.8	0.87	1.32	−3.54	4.06	−31.4%
VSS RRS	2.85	1.199	−3.3	3.22	0.687	−1.77	1.88	31.6%
Pole Plc	0.53	1.101	−3.6	2.02	0.918	−2.68	2.66	8.6%
Pole RRS	5.09	1.813	−5.85	4.17	1.348	−3.51	3.72	−34.2%
SS GPC	23.6	19.13	−36.6	37.1	2.269	−6.03	5.3	−125%

The following are results with a rudder rate of 15°/s.

Kynoc 90° Seas

Controller	RMS rudder angle	RMS yaw angle	Maximum yaw angle		RMS roll angle	Maximum roll angle		%PID
VSS RR	6.26	1.79	-4.63	5.67	1.9	-5.51	6.29	27.0%
Pole RR	9.41	2.42	-12.1	7	2.44	-8.81	9.71	6.3%
MV RR	10.1	1.38	-3.64	7.03	4.28	-11.8	12.6	-64.4%
SS GPC RR	8.35	2.2	-8.69	8.83	2.99	-11.5	12.6	-14.7%
PID	2	1.79	-4.53	5.39	2.6	-9.32	9.18	0.0%
Pole AP	5.91	0.56	-2.02	2	4.16	-13.9	15.1	-59.7%

Kynoc 45° Seas

Controller	RMS rudder angle	RMS yaw angle	Maximum yaw angles		RMS roll angle	Maximum roll angles		%PID
VSS RR	6.46	6.12	-17.8	19.1	3.77	-11.2	10.3	-69.8%
Pole RR	3.55	1.39	-4.6	13.6	2.23	-18	15.6	-0.6%
MV RR	3.26	2.26	-8.57	6.53	2.56	-7.01	8.27	-15.2%
SS GPC RR	2.68	0.85	-3.34	2.63	2.57	-7.81	8.3	-15.8%
PID	2.11	1.98	-6.4	5.65	2.22	-7.07	6.53	0.0%

Kynoc 60° Seas

Controller	RMS rudder angle	RMS yaw angle	Maximum yaw angle		RMS roll angle	Maximum roll angle		%PID
VSS RR	6.25	5.61	-19.8	17.7	3.33	-8.98	8.94	-40.6%
Pole RR	3.37	0.96	-3.33	5.71	1.84	-12.4	12.2	22.3%
MV RR	5.49	1.92	-6.45	6	4.34	-11.2	9.8	-83.6%
SS GPC RR	3.08	0.96	-4.32	4.27	3.37	-10.8	9.89	-42.4%
PID	2.17	1.96	-5.84	5.55	2.37	-5.88	8.7	0.0%
Pole AP	2.27	0.59	-2.79	2.01	2.38	-7.28	7.9	-0.5%

Kynoc 30° Seas

Controller	RMS rudder angle	RMS yaw angle	Maximum yaw angle		RMS roll angle	Maximum roll angle		%PID
VSS RR	4.19	1.61	−4.08	4.61	1.21	−3.52	3.73	9.5%
Pole RR	2.49	0.72	−2.69	2.7	1.3	−4.28	4.34	2.4%
MV RR	6.56	0.92	−4.34	3.06	2.1	−7.21	6.76	−57.5%
SS GPC RR	5.67	0.98	−4.9	2.99	1.71	−7.47	6.43	−28.5%
PID	1.7	1.48	−3.69	4.51	1.33	−4.79	4.07	0.0%
Pole AP	3.97	0.47	−2.44	1.98	1.54	−4.87	5.02	−15.5%

Eastward Ho 90° Seas

Controller	RMS rudder angle	RMS yaw angle	Maximum yaw angle		RMS roll angle	Maximum roll angle		%PID
VSS RR	12.6	2.13	−9.07	5.41	4.37	−12	11.8	0.7%
Pole RR	16.4	11.3	−33	31.2	4.81	−16.6	15.6	−9.5%
MV RR	15.9	8.11	−23.6	30.9	3.72	−11.1	11.8	15.4%
SS GPC RR	18.4	2.54	−7.94	10.4	4.07	−11.6	11.9	7.4%
PID	0.73	0.68	−2.37	1.81	4.39	−12	12.3	0.0%
Pole AP	0.46	0.98	−2.52	2.69	3.92	−12.1	11.4	10.7%

Eastward Ho 45° Seas

Controller	RMS rudder angle	RMS yaw angle	Maximum yaw angle		RMS roll angle	Maximum roll angle		%PID
VSS RR	4.12	2.25	−6.89	7.74	0.72	−2.47	2.03	11.0%
Pole RR	3.31	0.61	−2.41	1.65	0.71	−2.24	2.47	12.2%
MV RR	12.8	19.4	−53.2	55.2	2.31	−6.69	6.94	−186.5%
SS GPC RR	5.5	0.62	−2.65	3.3	2.12	−10.7	9.68	−162.6%
PID	1.59	1.54	−3.58	4.02	0.81	−2.35	2.5	0.0%
Pole AP	2.12	2.17	−6.7	4.55	0.83	−2.46	2.74	−3.6%

Eastward Ho 60° Seas

Controller	RMS rudder angle	RMS yaw angle	Maximum yaw angle		RMS roll angle	Maximum roll angle		%PID
VSS RR	5.46	3.53	−10.3	9.97	1.34	−4.1	3.74	20.1%
Pole RR	5.15	0.68	−1.9	3.18	1.23	−3.42	3.78	26.8%
MV RR	3.97	3.26	−12.6	8.62	1.83	−5.25	5.77	−9.0%
SS GPC RR	5.9	0.84	−4.58	4.57	2.96	−11.6	11.5	−76.3%
PID	2.04	1.97	−5.96	7.08	1.68	−5.43	5.67	0.0%
Pole AP	2.45	2.75	−9.56	7.76	1.81	−4.22	5.03	−7.8%

Eastward Ho 30° Seas

Controller	RMS rudder angle	RMS yaw angle	Maximum yaw angle		RMS roll angle	Maximum roll angle		%PID
VSS RR	4.65	1.38	−3.85	2.68	0.78	−2.62	2.02	19.8%
Pole RR	5.54	0.99	−2.87	3.89	0.98	−5.56	4.4	0.0%
MV RR	2.16	1.32	−2.69	2.89	1	−3.08	3.66	−1.8%
SS GPC RR	8.65	0.7	−2.96	2.89	2.29	−8.37	8.21	−134.2%
PID	0.92	0.88	−2.34	1.97	0.98	−3.06	3.38	0.0%
Pole AP	0.68	1.28	−2.97	2.93	0.92	−2.6	3.05	6.3%

94